

Durham Research Online

Deposited in DRO:

10 February 2015

Version of attached file:

Accepted Version

Peer-review status of attached file:

Peer-reviewed

Citation for published item:

Porter, S.J. and Selby, D. and Vyllinniskii, C. (2014) 'Characterising the nickel isotopic composition of organic-rich marine sediments.', *Chemical geology*, 387 . pp. 12-21.

Further information on publisher's website:

<http://dx.doi.org/10.1016/j.chemgeo.2014.07.017>

Publisher's copyright statement:

NOTICE: this is the author's version of a work that was accepted for publication in *Chemical Geology*. Changes resulting from the publishing process, such as peer review, editing, corrections, structural formatting, and other quality control mechanisms may not be reflected in this document. Changes may have been made to this work since it was submitted for publication. A definitive version was subsequently published in *Chemical Geology*, 387, 10 November 2014, 10.1016/j.chemgeo.2014.07.017.

Additional information:

Use policy

The full-text may be used and/or reproduced, and given to third parties in any format or medium, without prior permission or charge, for personal research or study, educational, or not-for-profit purposes provided that:

- a full bibliographic reference is made to the original source
- a [link](#) is made to the metadata record in DRO
- the full-text is not changed in any way

The full-text must not be sold in any format or medium without the formal permission of the copyright holders.

Please consult the [full DRO policy](#) for further details.

Manuscript Number: CHEMGE7765R1

Title: Characterising the nickel isotopic composition of organic-rich marine sediments

Article Type: Research Article

Keywords: Nickel isotope fractionation, Ni isotopes, $\delta^{60}\text{Ni}$, organic-rich marine sediments, Sinemurian-Pliensbachian GSSP, Exshaw Formation, redox

Corresponding Author: Dr. Sarah Porter, Ph.D.

Corresponding Author's Institution: Chemostrat Ltd

First Author: Sarah Porter, Ph.D.

Order of Authors: Sarah Porter, Ph.D.; David Selby; Vyllinniskii Cameron

Abstract: New Ni stable isotope data ($\delta^{60}\text{Ni}$) determined by double-spike MC-ICP-MS for two geologically distinct suites of organic-rich marine sediments from the Sinemurian-Pliensbachian (S-P) Global Stratotype Section and Point (GSSP; Robin Hood's Bay, UK) and the Devonian-Mississippian Exshaw Formation (West Canada Sedimentary Basin) is presented herein. These sediments yield $\delta^{60}\text{Ni}$ values of between 0.2 ‰ and 2.5 ‰, and predominantly have Ni isotopic compositions that are heavier than those of abiotic terrestrial and extraterrestrial samples (extraterrestrial and abiotic terrestrial samples (-0.1 ‰ and 0.4 ‰) (0.15 ‰ and 0.27 ‰), and in some cases present-day seawater (1.44 ‰) and dissolved Ni from riverine input (0.80 ‰). In addition, the observed degree of isotopic fractionation in the marine sediments is far greater than that of these other sample matrices. However, a strong similarity is exhibited between the $\delta^{60}\text{Ni}$ values of the organic-rich sediments studied here and those of ferromanganese crusts (0.9 to 2.5 ‰), suggesting that factors ubiquitous to the marine environment are likely to play a key role in the heightened level of isotopic fractionation in these sample matrices.

A lack of correlation between the Ni stable isotope compositions of the organic-rich sediments and Ni abundance, suggests that isotopic fractionation in these sediments is not controlled by uptake incorporation or enrichment of Ni during sediment accumulation. Further, no relationship is observed between $\delta^{60}\text{Ni}$ and TOC concentrations or bottom-water redox conditions, indicating that the organic carbon reservoir and levels of oxygenation at the sediment-water interface do not exert a primary control on Ni isotope fractionation in marine sediments. Following examination of these relationships, it is therefore more likely that the heavy Ni isotope compositions of marine sediments are controlled by the weathering environment and the dominant sources of dissolved Ni into the global ocean reservoir.

Characterising the nickel isotopic composition of organic-rich marine sediments

Sarah J. Porter^{1,2*}, David Selby¹, and Vyllinniskii Cameron³

¹ Department of Earth Sciences, Science Labs, Durham University, Durham, DH1 3LE, UK

² Chemostrat Ltd., Unit 1 Ravenscroft Court, Buttington Cross Enterprise Park, Welshpool, Powys, SY21 8SL, UK

³ Bristol Isotope Group, School of Earth Sciences, University of Bristol, Bristol BS8 1RJ, UK

*Corresponding author: Sarah J. Porter. Email: sarahporter@chemostrat.com; Tel.: +44(7889)838599

Keywords: Nickel isotope fractionation, Ni isotopes, $\delta^{60}\text{Ni}$, organic-rich marine sediments, Sinemurian-Pliensbachian GSSP, Exshaw Formation, redox

Abstract

New Ni stable isotope data ($\delta^{60}\text{Ni}$) determined by double-spike MC-ICP-MS for two geologically distinct suites of organic-rich marine sediments from the Sinemurian-Pliensbachian (S-P) Global Stratotype Section and Point (GSSP-~~;~~ Robin Hood's Bay, UK) and the Devonian-Mississippian Exshaw Formation (West Canada Sedimentary Basin) is presented herein. These sediments yield $\delta^{60}\text{Ni}$ values of between 0.2 ‰ and 2.5 ‰, and predominantly have Ni isotopic compositions that are heavier than those of abiotic terrestrial and extraterrestrial samples ~~—extraterrestrial and abiotic terrestrial samples (–0.1 ‰ and –0.4 ‰)~~ (0.15 ‰ and 0.27 ‰), and in some cases present-day seawater (1.44 ‰) and dissolved Ni from riverine input (0.80 ‰). In addition, the observed degree of isotopic fractionation in the marine sediments is far greater than that of these other sample matrices. However, a strong similarity is exhibited between the $\delta^{60}\text{Ni}$ values of the organic-rich sediments studied here and those of ferromanganese crusts (0.9 to 2.5 ‰), suggesting that factors ubiquitous to

the marine environment are likely to play a key role in the heightened level of isotopic fractionation in these sample matrices.

A lack of correlation between the Ni stable isotope compositions of the organic-rich sediments and Ni abundance, suggests that isotopic fractionation in these sediments is not controlled by ~~uptake~~incorporation or enrichment of Ni during sediment accumulation. Further, no relationship is observed between $\delta^{60}\text{Ni}$ and TOC concentrations or bottom-water redox conditions, indicating that the organic carbon reservoir and levels of oxygenation at the sediment-water interface do not exert a primary control on Ni isotope fractionation in marine sediments. Following examination of these relationships, it is therefore more likely that the heavy Ni isotope compositions of marine sediments are controlled by the weathering environment and the dominant sources of dissolved Ni into the global ocean reservoir.

58

59

60

61 1. Introduction

62

63 For several decades previous investigations of Ni isotopes have focused
64 predominantly on characterising radiogenic isotopic fractionation in extraterrestrial
65 materials, with a view to enhancing our understanding of planetary processes and
66 the isotopic composition of the early Solar System (eg. Kohman and Robison, 1980;
67 Morand and ~~Allegre~~Allègre, 1983; Shimamura and Lugmair, 1983; Birck and Lugmair,
68 1988; Herzog et al., 1994; Xue et al., 1995; Quitté et al., 2006; Cook et al., 2007;
69 Moynier et al., 2007; Chen et al., 2009). Further, the role of Ni as a bioessential trace
70 metal (eg. Frausto da Silva and Williams, 2001; Cameron et al., 2007; 2009) has led
71 to the recognition that the stable isotopes of Ni may have the potential to be utilised
72 as a powerful biological tool for studies of early life on Earth (Cameron et al., 2009;
73 2012).

74 In addition to its role in cosmochemical and biochemical investigations, the
75 potential of Ni to significantly enhance our understanding of organic-rich
76 sedimentary environments and to provide a powerful geological tracer in the
77 petroleum realm has been recognised, following pioneering work by Lewan and
78 Maynard (1982) and Lewan (1984) (eg. Ellrich et al., 1985; Manning et al., 1991;
79 Alberdi and Lafargue, 1993; López et al., 1995). However, these studies focused on
80 the elemental distribution of Ni rather than on its isotopic characterisation, and as
81 such, no study currently exists that evaluates the behaviour of Ni stable isotopes in

organic-rich sediments or indeed within a stratigraphic profile. This can be attributed to Ni being a relatively newly investigated system, together with the difficulty associated with purifying Ni from such complex sample matrices, that has only recently been overcome through advancements in analytical and mass spectrometry techniques (eg. Gall et al., 2012; Cameron and Vance, 2014).

Until now, Ni stable isotope systematics in organic-rich sedimentary matrices have not been investigated. Indeed, it is only recently that the Ni isotopic composition of seawater and the sources of Ni to the global oceanic reservoir have been determined (e.g. Cameron and Vance, 2014; Gall et al., 2013). Present-day seawater has an average $\delta^{60}\text{Ni}$ value of 1.44 ± 0.15 ‰, with apparent global isotopic homogeneity (Cameron and Vance, 2014). The oceanic residence time of Ni has been calculated as ~30 kyr (Cameron and Vance, 2014), which is significantly longer than the mixing time of the global oceans (~2,000 yrs; Palmer et al., 1988). This would be sufficient for the ocean to have an isotopically homogenous Ni composition. Cameron et al. (2014) also demonstrate that draw-down of Ni from the surface to deep ocean during trace metal cycling is not accompanied by isotopic fractionation, thus further suggesting that the ~~global~~modern ocean is isotopically homogenous. In the absence of any Ni isotope studies on banded iron formation and shale datasets, it is difficult to speculate on processes occurring in an ancient ocean. However, examination of Ni/Fe data from banded iron formations and extrapolated maximum dissolved Ni concentration values in sea water through time (Konhauser et al., 2009), demonstrates that dissolved nickel concentrations may have reached present day values by ~550 Ma. As such, given the age of the sediments being studied herein (~190-360 Ma), it is appropriate to use what we know regarding modern ocean

circulation and fractionation processes to hypothesise about processes acting in the ancient oceans.

The predominant input of dissolved Ni to the oceans occurs via riverine influx, which has been suggested to yield an annual discharge- and concentration-weighted $\delta^{60}\text{Ni}$ average of +0.80 ‰ (Cameron and Vance, 2014). Significant variability in the riverine isotopic composition has been observed (+0.29 to +1.34 ‰), which has been attributed to isotopic fractionation of Ni during weathering of continental crust, resulting in heavier $\delta^{60}\text{Ni}$ values in rivers and seawater. In addition, mineral dust and volcanic ash also contribute to the oceanic Ni budget (Li and Schoonmaker, 2003), as well as hydrothermal vent fluids ($\delta^{60}\text{Ni} = 1.5$ ‰; Gall et al., 2012).

Herein we present the first attempt at creating a Ni isotope stratigraphic profile for an organic-rich sedimentary succession. The marine section across the Sinemurian-Pliensbachian Global Stratotype Section and Point (GSSP), Robin Hood's Bay, UK, is ideally suited to the present study, as it well understood biostratigraphically (Hesselbo et al., 2000; Meister et al., 2006) and has been previously characterised using other isotope stratigraphy techniques, including strontium ($^{87}\text{Sr}/^{86}\text{Sr}$; Jones et al., 1994; Hesselbo et al., 2000), oxygen ($\delta^{18}\text{O}$), carbon ($\delta^{13}\text{C}$) (Hesselbo et al., 2000), and Re-Os isotopes (Porter et al., 2013). The section is also consistently thermally immature (the rocks have not been subjected to enough heat or pressure to convert any kerogens present to hydrocarbons), thereby eliminating any potential effects of thermal maturation on the Ni isotope signature. In addition, to draw comparison between the isotopic composition of samples of different depositional ages and environments, we present Ni isotope data from a

selection of thermally immature black shale samples from a core of the Exshaw Formation, Canada.

To accurately assess and interpret any stratigraphic variation of Ni isotopes in the Robin Hood's Bay section and Exshaw Formation samples, it is critical to determine whether any fluctuations in paleoredox conditions occur. Nickel primarily occupies one oxidation state in the natural environment (Ni^{2+}), suggesting that it is not redox sensitive. However, its preferential association with redox-sensitive metallo-organic complexes (porphyrins) in organic-rich sediments (Lewan and Maynard, 1982) indicates that certainly within these sample matrices, redox conditions at the time of sediment deposition may directly impact the degree of enrichment or depletion of Ni. Herein, paleoredox conditions have been established for the Sinemurian-Pliensbachian GSSP section and the Exshaw Formation sample suite. Although one previous study (Dewaker et al., 2000) provides a preliminary dataset for the Ni isotope composition of sediments from 3 different basins, our understanding of the behaviour of Ni isotope systematics within organic-rich sediments is currently non-existent. Further, advancements in analytical techniques over the past decade suggest that the methodology employed by Dewaker et al. (2000) may not have been optimal for Ni separation or Ni stable isotope analysis.

This paper presents the first detailed study of nickel stable isotope systematics in organic-rich marine sediments. Analysis of marine sediments of different depositional ages and from two geologically distinct settings, the Sinemurian-Pliensbachian boundary (UK) and the Devonian-Mississippian Exshaw Formation (Canada), yields comparable Ni isotope compositional values for both sites. These samples provide insight into the incorporation~~uptake~~ of Ni into ocean

sediments, and allow evaluation of the contribution of the various dissolved Ni fluxes to the seawater during these time periods.

2. Geological Setting

2.1 The Sinemurian-Pliensbachian boundary GSSP, Robin Hood's Bay, UK

The Sinemurian-Pliensbachian boundary, established from the succession's complete ammonite assemblages (Spath, 1923; Dean et al., 1961; Hesselbo et al., 2000; Meister et al., 2006), occurs in the Pyritous Shales of the Redcar Mudstone Formation within the Lias Group at Robin Hood's Bay (Powell, 1984; Fig. 1). At this point in the Early Jurassic, Robin Hood's Bay was positioned on the margins of a shallow epicontinental sea (eg. Dera et al., 2009) that covered most of Northern Europe, including Britain, during the Mesozoic (Sellwood and Jenkyns, 1975). The facies changes across the boundary, from pale siliceous to finer, more organic-rich mudstones (Fig. 2), indicate an overall relative increase in sea level of at least regional extent (eg. Hesselbo et al., 2000; Meister et al., 2006; Porter et al., 2013).

The age for the base of the Pliensbachian has been defined by the Geological Time Scale (GTS) 2012 as 189.6 ± 1.5 Ma (Gradstein et al., 2012), derived from cycle-scaled linear Sr trends and ammonite occurrences (as noted above; also includes the lowest occurrence of *Bifericeras donovani*; Gradstein et al., 2012).

2.2 Exshaw Formation, West Canada Sedimentary Basin (WCSB)

The West Canada Sedimentary Basin (WCSB) trends approximately NW-SE between the Canadian Shield to the East and the Western Cordillera to the West (Piggott and Lines, 1992). Within the WCSB lies the Exshaw Formation, a thin but laterally continuous unit (2-12 m thick; Leenheer, 1984; Creaney and Allan, 1991). The Exshaw Formation in south-west and western Alberta (Fig. 3) comprises a lower member of organic-rich mudrocks and black shales which rest with minor disconformity upon Upper Devonian carbonate strata (Richards et al., 1999), and are abruptly to gradationally overlain by bioturbated shelf siltstones (Caplan and Bustin, 1998, 1999; Creaser et al., 2002). The depositional interval of the lower black shale unit is well constrained biostratigraphically; between the *expansa* and *duplicata* zones of Late Famennian to Early Tournaisian time (over a maximum time period of ~363 – 360 Ma; Caplan and Bustin, 1998). These lower black shales are dark grey, bituminous, relatively thin (consistently between 3-5 m; Meijer et al., 1994) and widespread (Meijer et al., 1994). The Devonian-Mississippian boundary (Exshaw-type section at Jura Creek, ~80 km west of Calgary, Alberta, Canada) represents the boundary between the upper calcareous and lower non-calcareous black shale units (Richards and Higgins, 1988). Selby and Creaser (2005) provide an absolute Model 1 Re-Os age for this boundary, and thus the top of the lower black shale unit, of 361.3 ± 2.4 Ma. In addition, U-Pb monazite data from a tuff horizon close to the base of the lower black shale member constrains an absolute depositional age for this unit of 363.4 ± 0.4 Ma (Richards et al., 2002). Deposition at this time represents part of a continent-wide Famennian-Tournaisian black shale event, and in turn, a possible ocean anoxic event (Piggott and Lines, 1992).

3. Sampling

A set of 32 samples (SP7-09 to SP39-09) was collected from the Pyritous Shales Member of the Redcar Mudstone Formation, along a 6 m vertical section bracketing the Sinemurian–Pliensbachian boundary (sample SP22-09) at Robin Hood’s Bay (Fig. 2). This marine sequence contains a rich fauna of ammonites both above and below the boundary interval (Hesselbo et al., 2000). Total organic carbon analysis was conducted on all samples, with a consistent sampling interval of ~20 cm for 3 m above and 3 m below the boundary from Beds 69–75 (except within Bed 72, where a smaller sampling interval of ~15 cm was used). Of these samples, 14 were analysed for Ni isotopes at a sampling interval of ~40 cm (Fig. 2).

Four samples from the Lower member of the Exshaw Formation were collected from the Alberta Energy and Utilities Board, Core Research Centre, Calgary (Fig. 3). The samples were taken from core 3-19-80-23W5, as detailed in Piggot and Lines (1992) and Creaser et al. (2002). All samples are thermally immature, fine-grained black shales containing very thin parallel and undulating laminations, and showing no evidence of post-depositional disturbance. Drill core samples were obtained to avoid any potential effects of surface weathering, including loss of organic matter (Peucker-Ehrenbrink and Hannigan, 2000). Further, edges of the core were polished and where possible samples were taken from the central part of the core.

4. Analytical Protocol

4.1 Trace element abundance and TOC

The elements V, Cr, Ni and Co were analysed in this study in order to look at relative changes of depositional redox conditions in the sediments of interest.

Samples were prepared for trace element analysis at the Durham Geochemistry Group (University of Durham, UK) following the method of Ottley et al., (2003). Sample powders (~100 mg) were digested in a 4:1 solution of 29 N HF and 16 N HNO₃ at ~150 °C for 48 hrs. Samples were then evaporated to near rather than total dryness, to avoid stabilisation of insoluble fluorides (Ottley et al., 2003). This was followed by the addition of 1 ml 16 N HNO₃ and evaporation to near dryness. The previous stage was repeated before the addition of 2.5 ml 16 N HNO₃ and ~10 ml 18MΩ water to create a ~4 N HNO₃ solution. Sample beakers were capped and heated on the hotplate overnight at ~100 °C. Once cooled, 1 ml of 1 ppm internal Re and Rh spike was added to the samples (to yield 20 ppb Re and Rh in the final analyte solution) before dilution up to 50 ml with MQ, yielding a ~0.5 N HNO₃ solution. Prior to analysis, samples were diluted 10-fold by taking 1 ml from the 50 ml solution and diluting it to 10 ml using 0.5 N HNO₃. Samples were then analysed using the Thermo X-Series Quadrupole Inductively Coupled Plasma Mass Spectrometer (ICP-MS).

—Replicate analyses of USGS International Reference Materials (RMs) AGV-1, BHVO-1 and W-2 ~~and synthetic standards solutions for Mo (10, 20 and 30 ppb solutions)~~ were conducted for calibration per sample set.

Total organic carbon measurements were performed at Durham University using a Costech Elemental Analyser (ECS 4010) coupled to a ThermoFinnigan Delta V Advantage. Total organic carbon was obtained as part of the isotopic analysis ($\delta^{13}\text{C}_{\text{org}}$) using an internal standard (Glutamic Acid, 40.82 % C). Data accuracy was monitored through routine analyses of in-house standards, which are stringently calibrated against international standards (eg. USGS 40, USGS 24, IAEA 600, IAEA CH6).

4.2 Nickel stable isotopes

All Ni isotope analyses were conducted at the University of Bristol. Samples (~100 mg) were digested in closed PFA Beakers (Savillex, Minnetonka, MN) in a mixture of concentrated HF and HNO_3 (3:1) at 140 °C for 48 hrs. Dried samples were treated further with 7 N HCl. Chemical separation, purification and analyses of Ni isotopes was carried out as described in detail in Cameron et al. (2009) and Cameron and Vance (2014),—2013). Briefly, sample aliquots were spiked and allowed to equilibrate under heating in closed vials overnight. This was followed by drying down and treatment with 7 N HCl + H_2O_2 . The spiked samples were then put through a 3-stage column procedure that in turn removes Fe and Zn, separates Ni from the bulk sample matrix, and final purification to remove any residual Fe and Zn. The first ion-exchange column (AG MP-1M, Bio-Rad) is used to remove Fe and Zn. The dried samples are then taken up in 1M HCl/1 M ammonium citrate, and the pH adjusted to 8–9 before loading onto columns filled with Ni resin (Eichrom Technologies). This step separates Ni while removing all other matrix elements in the sample. After oxidation to remove Ni-bound DMG, the samples are finally put through a third

[column, which is a repeat of the first anion column, to clean up any residual Fe and Zn.](#)

All analyses were conducted in low resolution mode using a ThermoFinnigan Neptune multi-collector (MC) ICP-MS coupled to an Aridus desolvating nebuliser system (CETAC, Omaha, NE, USA). Samples were introduced in 2% HNO₃ via a CPI PFA nebuliser (50 µl/minute) and spray chamber. Prior to isotopic analysis, the ⁵⁶Fe/⁵⁸Ni ratio was manually checked in high resolution mode in all samples so that any potential isobaric interference from residual sample ⁵⁸Fe could be applied as a correction to Ni mass 58. Relative to the propagated internal uncertainty on δ⁶⁰Ni, the correction was insignificant. Additionally, a small amount of N₂ was introduced to the Aridus sweep gas to reduce a potential interference from ⁴⁰Ar¹⁸O at mass 58. To mitigate inaccuracies in the δ⁶⁰Ni brought on by any instrumental variations, measurements of the pure NIST SRM986 standard were made throughout the analytical session. The reproducibility and accuracy of all isotope ratios were monitored further by measurement of mixtures of the SRM986 standard with the double-spike. All isotopes were measured simultaneously in static mode using a multiple Faraday collector array. All Ni data are reported relative to NIST SRM986, in the standard delta notation ($\delta^{60}\text{Ni} = [({}^{60}\text{Ni}/{}^{58}\text{Ni})_{\text{sample}}/({}^{60}\text{Ni}/{}^{58}\text{Ni})_{\text{NISTSRM986}}]-1] \times 1000$), with all uncertainties reported to the 2σ level.

5. Results

5.1 Trace elements and TOC

The trace element ratios Ni/Co, V/Cr and V/(V+Ni) have been utilised by previous studies to evaluate paleoredox conditions at the time of sediment deposition (eg. Hatch and Leventhal, 1992; Jones and Manning, 1994; Schovsbo, 2001; Rimmer, 2004). Both Ni and V occur in highly stable tetrapyrrole complexes that are originally derived from chlorophyll and are preferentially preserved under anoxic conditions (Lewan and Maynard, 1982). When organic matter has been extensively exposed to aerobic conditions, preservation of these tetrapyrrole complexes will be low and subsequently the organic matter will have low Ni and V contents. Chromium is not influenced by redox conditions, and thus because of its association with just the detrital fraction and not the organic matter (Dill, 1986), high V/Cr values (>2) are indicative of anoxic conditions. Both Ni and Co are found in pyrite (in addition to the occurrence of Ni in porphyrins), but high Ni/Co values are associated with anoxic conditions (Jones and Manning, 1994). The relationship between these ratios and depositional redox conditions are summarised in Table 1.

The abundances of Ni, Co, V, Cr and TOC for all samples from Robin Hood's Bay and the Exshaw Formation, are presented in Table 2. Both the Ni/Co and V/Cr indices for Robin Hood's Bay show that these sediments were deposited under predominantly oxic conditions. Good agreement is observed between both the Ni/Co and V/Cr indices for Robin Hood's Bay, which show that the samples were deposited under predominantly oxic conditions. However, there is significant disagreement between these ratios and the V/(V+Ni) index. Values for V/(V+Ni) range from ~0.51 – 0.89 and indicate that anoxic conditions prevailed across the Sinemurian-Pliensbachian boundary. Further, six samples suggest that bottom-water

circulation ceased and that conditions became euxinic intermittently between ~2.6 m above the boundary and ~1.9 m below it (Table 2).

The Ni/Co ratio in the Exshaw Formation sediments ranges from 13.8 – 21.4, with all four samples falling within the suboxic-anoxic parameter (Table 2). Similarly, the V/(V+Ni) ratio indicates that three of the samples were deposited under suboxic-anoxic conditions (SP8-10, SP10-10 and SP13-10; values of 0.67, 0.69 and 0.67, respectively). However, whilst V/Cr values of 7.2 and 9.0 suggest a suboxic-anoxic depositional environment for Exshaw Formation samples SP10-10 and SP13-10, respectively, this ratio also yields values that are representative of dysoxic conditions for samples SP8-10 and SP9-10 (2.0 and 2.1, respectively).

Total organic carbon content is generally low in the Sinemurian-Pliensbachian sediments, varying from ~0.53 – 2.46 wt. % (Table 2; Fig. 4). The data shows only slight variation prior to the boundary (~0.57 – 0.86 wt. %; Fig. 4), but an overall gradual increase above the boundary (from ~0.58 – 2.46 wt. %; Fig. 4). Total organic carbon values in the Exshaw Formation samples range from 1.2 – 11 wt. %.

5.2 Nickel stable isotopes

New Ni stable isotope data for a select suite of the organic-rich sediments at Robin Hood's Bay is presented (see Table 3). From the base of Bed 71 the sampling interval for Ni isotope analysis is ~40 cm (Fig. 2). A profile of $\delta^{60}\text{Ni}$ values for the section is shown alongside Ni concentration and TOC for comparison (Fig. 4).

The $\delta^{60}\text{Ni}$ of these samples is extremely variable, ranging from 0.28 ± 0.05 – 1.60 ± 0.05 ‰ (Fig. 4; Table 3). Two noticeable peaks in $\delta^{60}\text{Ni}$ values are observed 0.8 m above and 2.1 m below the Sinemurian-Pliensbachian boundary (1.26 ± 0.05 ‰

and 1.60 ± 0.05 ‰, respectively) that approximately correlate with the tops of beds 70 and 74. The greatest range in $\delta^{60}\text{Ni}$ values occurs below the boundary (~ 1.32 ‰), compared to a range of ~ 0.97 ‰ above the boundary (Fig. 4). In this section and dataset there is no apparent relationship between the degree of Ni isotope fractionation and depositional redox conditions, TOC or stratigraphic height (Fig. 4).

Nickel stable isotope data for the Exshaw Formation is also presented in Table 3. The $\delta^{60}\text{Ni}$ values in these samples range from 0.46 ± 0.04 to 2.50 ± 0.04 ‰ (Table 3). As with the Robin Hood's Bay section, no relationship exists between $\delta^{60}\text{Ni}$ and sample depth or between $\delta^{60}\text{Ni}$ and depositional redox conditions, TOC or stratigraphic position (Fig. 4).

6. Discussion

6.1. Evaluating the suitability of $V/(V+Ni)$ as a redox proxy: How applicable is it?

The Ni/Co and V/Cr redox indices are recommended by a number of workers as the most reliable of the paleo-environmental proxies (eg. Jones and Manning, 1994; Rimmer, 2004), and have been used by several studies to provide accurate and consistent evaluations of paleoredox conditions at the time of sediment deposition (eg. Rimmer, 2004; Selby et al., 2009; this study). However, this study finds that there is significant disagreement between these indices and the $V/(V+Ni)$ index. For Robin Hood's Bay, the latter index suggests that the sediments were deposited in predominantly suboxic-anoxic bottom-waters, with intermittent euxinic periods. However, both the V/Cr and Ni/Co ratios indicate that the Robin Hood's Bay samples

were deposited under largely oxic condition. Such disparity between the redox indices is also noted by both Rimmer (2004) and Selby et al. (2009), who observe that the $V/(V+Ni)$ index suggests suboxic-anoxic conditions for sediments otherwise indicated to have been deposited under oxic conditions by the V/Cr and Ni/Co ratios.

Preliminary work by Lewan and Maynard (1982) and Lewan (1984) suggested that redox potential was a dominant control on the wide range of $V/(V+Ni)$ values observed in petroleum source rocks and oils. Following this, Hatch and Leventhal (1992) were the first to develop and utilise the $V/(V+Ni)$ index as a measure of relative redox potential in organic-rich sediments. Their study focused on applying this index specifically to marine black shales in the Pennsylvanian Stark Shale Member of the Dennis Limestone, Wabaunsee County, Kansas, USA (Hatch and Leventhal, 1992). Therefore, the ranges they defined for the $V/(V+Ni)$ ratio and the associated redox conditions (summarised in Table 1), are applicable to this specific geological basin and are sensitive to localised geochemical variations therein.

Hatch and Leventhal (1992) show that for the Stark Shale Member, with the exception of two outliers, low TOC values (<2.5 wt. %) correspond to $V/(V+Ni)$ values <0.75 , and samples containing greater TOC (>7.5 wt. %) have corresponding higher $V/(V+Ni)$ values (0.75; Fig. 5). However, this relationship is not observed in the majority of the Sinemurian-Pliensbachian or Exshaw Formation sediments, with samples containing low TOC providing a range in $V/(V+Ni)$ data from $\sim 0.33 - 0.89$.

This immediately indicates that there are significant geochemical differences between these three geological sites. ~~have differing geochemical frameworks.~~ This may be due to differences in both geological age and stratigraphy, with the Stark Shale Member (Late Carboniferous) being a darker grey, non-sandy shale with higher

TOC content (Hatch and Leventhal, 1992). As such, this comparison suggests that the redox index $V/(V+Ni)$, originally developed for a specific geological basin, may not be applicable to other geological sites, particularly those that possess differing geological and geochemical characteristics. Factors that may have a profound effect upon the applicability of such a threshold from one study to another include: differences in the influx of nutrients and trace elements, type and relative amounts of organic matter, and degrees of oceanic mixing (~~eg., eg.~~ Rimmer, 2004). However, these are preliminary findings from a small dataset and further investigation is recommended. In agreement with Rimmer (2004), this study therefore suggests that caution should be taken when applying redox indices established by other studies for ~~specific-single~~ geological sites.

6.2. Nickel stable isotope fractionation in marine sediments

Nickel stable isotope data for the Exshaw Formation and the Sinemurian-Pliensbachian GSSP is presented in Table 3 and Figure 6, and is the first to be obtained for a suite of organic-rich marine sediments. The Exshaw Formation shales define a realm of $\delta^{60}Ni$ values of 0.46 ± 0.04 to 2.50 ± 0.04 ‰ (a range of ~ 2.04 ‰; Fig. 6). This range overlaps with, and is comparable to the $\delta^{60}Ni$ data for the Sinemurian-Pliensbachian boundary GSSP (0.28 ± 0.05 to 1.60 ± 0.05 ‰; ~ 1.32 ‰; Fig. 6). Although there are currently no estimations for the Ni isotopic composition of the palaeo-ocean, the present-day global seawater $\delta^{60}Ni$ value has been constrained as 1.44 ± 0.15 ‰ (Cameron and Vance, 2014). This value lies within the $\delta^{60}Ni$ range of the marine sediments (Fig. 6; this study). Draw-down of Ni through the water column does not induce isotopic fractionation, and as such, the Ni stable

isotope composition of the ocean is assumed to be homogenous (Cameron and Vance, 2014). However, the Ni stable isotope composition of the organic-rich sediments is far from homogenous, with $\delta^{60}\text{Ni}$ values that are either significantly lighter or heavier than the present-day seawater $\delta^{60}\text{Ni}$ value (Fig. 6). Assuming that global ocean homogeneity has persisted throughout geological time, the fractionation observed in the marine sediments must therefore be recording the substantially variable isotopic compositions of the sources of dissolved Ni into the oceans.

This preliminary study presents Ni isotope and Ni concentration data from bulk sample analysis. To assess what fraction of the selected metals may be authigenic versus lithogenic, Table 4 presents Ni concentration data from this study, and from average shale and average upper continental crust. It is clear from this that the authigenic contribution of Ni in these samples is < 50 % (Table 4), suggesting that > 50 % of the sample is represented by the lithogenic fraction.

For both sample sets, no correlation is observed between $\delta^{60}\text{Ni}$ and Ni abundance, indicating that the level of Ni isotope fractionation in ~~bulk~~^{the} marine sediments here is not directly controlled by the degree of Ni enrichment. Similarly, no relationship exists between $\delta^{60}\text{Ni}$ and redox for either sample set, suggesting that the level of isotopic fractionation is not solely dictated by the bottom water redox conditions at the time of sediment deposition. However, although it is currently poorly understood, it is interesting to consider whether or not the degree of organic matter preservation could have an effect on the observed isotopic fractionation within the sediments. The samples used for Ni isotope analysis across the Sinemurian-Pliensbachian boundary were deposited in predominantly oxic

conditions (using the Ni/Co and V/Cr ratios). The tetrapyrrole complexes known to hold the majority of ~~the~~ Ni in organic matter are poorly preserved under these conditions (Lewan and Maynard, 1982). As such, assuming break down of these complexes is heterogeneous, and that it does not result in the preferential loss of a particular isotope of Ni, this lack of preservation may at least partially contribute to the observed Ni isotope fractionation in these sediments.

In addition, no correlation is seen between $\delta^{60}\text{Ni}$ and TOC concentration in these samples, indicating that Ni isotope fractionation is not dependent on the concentration of organic matter in these sediments. However, all samples in this study have TOC contents of <3.0 wt. % (Table 3; apart from Exshaw Fm. sample SP10-10; 11.05 wt. %). As such, to further investigate the relationship between Ni fractionation and the organic carbon reservoir, work should be conducted on samples containing more varied and greater levels of TOC.

6.3. Fractionation of nickel stable isotopes in marine organic-rich sediments vs. terrestrial samples, extra-terrestrial samples and ferromanganese crusts

Marine sediments from the Exshaw Formation and Sinemurian-Pliensbachian GSSP yield a comparable range in $\delta^{60}\text{Ni}$ values (0.5-2.5 ‰ and 0.3-1.6 ‰, respectively; Fig. 6). Figure 6 compares these Ni isotopic values with that of bulk Earth and extraterrestrial samples (Cameron et al., 2009), including meteorites (0.2 ‰ to 0.4 ‰), basalts (0 to 0.3 ‰) and continental sediments (0 to 0.2 ‰). It is clear that these samples are significantly isotopically lighter than the organic-rich sediments (this study). In addition, Ni stable isotope fractionation occurs to a much greater degree in the sedimentary marine environment. Despite this though, there is

minimal overlap between the $\delta^{60}\text{Ni}$ values for the organic-rich sediments and those of the abiotic terrestrial and extraterrestrial samples (Fig. 6).

The reasons for the heightened isotopic fractionation in marine sediments are currently poorly understood due to an extremely limited sample database. However, the complexity of the marine environment is likely to play a critical role in this. With assumed ocean isotopic homogeneity (Cameron and Vance, 2014), the sources of dissolved Ni into seawater must exert a substantial control on the observed degree of isotopic fractionation. This may be partially attributed to the variability of the Ni isotope composition of the dissolved phase of rivers, which are a dominant source of Ni to the global oceans ($\delta^{60}\text{Ni} = 0.29$ to 1.34 ‰; Cameron and Vance, 2014). The heavier isotope composition of this fraction relative to silicates and continental sediments (0 ‰ to 0.3 ‰; Cameron et al., 2009) likely reflects isotopic fractionation induced by the weathering environment during riverine transport (Cameron and Vance, 2014).

However, this study demonstrates that the Ni isotopic composition of organic-rich marine sediments ($\delta^{60}\text{Ni} = 0.28$ to 2.50 ‰; this study) are significantly heavier than that of the riverine source (average $\delta^{60}\text{Ni} = 0.80$ ‰; Cameron and Vance, 2014). This is also the case for the dissolved phase of present-day seawater ($\delta^{60}\text{Ni} = 1.44 \pm 0.15$ ‰; Cameron and Vance, 2014). To reconcile this, there must therefore be either an additional input that is isotopically heavier than the riverine source (Cameron and Vance, 2014).

Dissolved trace metals are often removed from the water column via adsorption to mineral surfaces as they are incorporated into the sediment. The adsorption process, in particular to Mn and Fe oxyhydroxides, is known to induce

isotopic fraction in a number of stable isotope systems, including Mo and U (Brennecke et al., 2011; Wasylenki et al., 2008; 2011). Sorption to Fe-Mn oxides is the main output of Ni from the oceans (Cameron and Vance, 2014), and more recently, this fractionation effect has also been revealed in the Ni stable isotope system (Wasylenki et al., 2014). In addition, experiments focusing on the adsorption and co-precipitation of Ni with oxyhydroxide phases (Wasylenki et al., 2014) have demonstrated that isotopically light Ni is retained by these phases whilst isotopically heavy Ni is mobilised. This therefore leads to an enrichment of isotopically heavy Ni in the dissolved riverine load (Wasylenki et al., 2014).

~~Further,~~ Nickel stable isotope data for ferromanganese crusts (0.9-2.5 ‰; Gall et al., 2013) shows that their isotopic composition is comparable to that of the marine organic-rich sediments discussed herein. Following analysis of ferromanganese crusts in proximity to hydrothermal sources, Gall et al. (2013) suggest that hydrothermal fluids may have a Ni stable isotope composition of ~ 1.5 ‰. Thus hydrothermal sources may be contributing to the isotopic composition noted in the marine sediments herein.

— However, both marine sediments (this study) and ferromanganese crusts (Gall et al., 2013) are at least in part recording isotopic fractionation from a source that is isotopically heavier than riverine and hydrothermal Ni influxes. As continental weathering is a primary source of Ni to the global oceans, it is likely that weathering-induced isotope fractionation could account for the isotopically heavy Ni composition of organic-rich marine sediments. Further, the heavy Ni isotope signature observed in these sediments may reflect the contribution of heavy dissolved Ni to the oceans following retention of the lighter Ni isotopes during

weathering of oxyhydroxide phases (eg. Wasylenki et al., 2014). In support of this, analysis of ferromanganese crusts at varying distances from the continental shelf (Gall et al., 2013) demonstrates that crusts growing in proximity to a continental shelf contain the heaviest Ni isotope compositions. However, although weathering does affect the isotopic composition of marine sediments, the effects resulting from additional factors such as riverine particulates, ~~Mn-oxides~~ and organic compounds have yet to be constrained (Cameron and Vance, 2014).

In addition, following examination of Ni isotope data from microorganisms ($\delta^{60}\text{Ni} = \sim 0.0$ to -1.6 ‰; Cameron et al., 2009), it can be noted that the Ni isotope ratios in the organic-rich sediments herein ($\delta^{60}\text{Ni} = \sim 0.28 - 2.50$ ‰) appear to have been driven in the opposite direction to those of the microorganisms. Whilst the causes of Ni isotope fractionation in these sediments are currently poorly understood, it appears that there is a fractionation effect associated with the Ni isotope system that may have parallels to the carbon isotope system, with the microorganisms taking up isotopically lighter Ni, thus potentially leaving behind an isotopically heavier Ni isotope signature in the sediment. Although it is impossible to draw a definitive conclusion from the current dataset, this study suggests that microorganisms and organic matter may play a key role in our understanding of Ni isotope fractionation (in a similar manner to the rhenium-osmium isotope system; Cumming et al., 2012; Harris et al., 2013) in organic-rich marine sediments, and as such, the importance of further investigation is emphasised.

7. Conclusions

This first investigation into the Ni stable isotope composition of organic-rich marine sediments from two distinct basins has yielded a number of key observations, outlined below.

1. This preliminary dataset indicates that organic-rich sediments have a Ni stable isotope composition ($\delta^{60}\text{Ni}$) of 0.28 to 2.50 ‰.

2. No relationship is observed between the Ni stable isotope composition of the organic-rich sediments and TOC, suggesting that fractionation is not determined by changes in the organic carbon reservoir.

3. Similarly, there is no correlation between $\delta^{60}\text{Ni}$ and Ni abundance or bottom-water redox conditions, suggesting that the process of Ni uptake and enrichment at the sediment-water interface, and the degree of oxygenation in the water-column do not exert primary control on isotopic fractionation.

24. The Ni isotope composition of marine sediments is substantially heavier and isotopically distinct to those of abiotic terrestrial and extraterrestrial samples ($\delta^{60}\text{Ni}$ values of -0.1 to 0.3 ‰; Cameron et al., 2009).

35. Ni isotopes in marine sediments are isotopically heavier than those in present-day seawater and rivers ($\delta^{60}\text{Ni} = 1.44 \pm 0.15$ ‰ and 0.29 to 1.34~~0.80~~ ‰, respectively;

Cameron and Vance, 2014)-, indicating input of an isotopically heavier source of Ni to the ocean.

~~46.~~ The observed range of $\delta^{60}\text{Ni}$ values in marine sediments is comparable to that of ferromanganese crusts (0.9 to 2.5 ‰; Gall et al., 2013). Adsorption of Ni to Fe-Mn oxyhydroxides results in the retention of isotopically light Ni and the mobilisation of isotopically heavier Ni during oxidative weathering (Wasylenki et al., 2014). Subsequently, the dissolved riverine load is enriched in heavier Ni. It is therefore probable that isotopic fractionation driven by the weathering environment plays a key role in yielding the range of $\delta^{60}\text{Ni}$ values that are observed in marine sediments.

~~5. No relationship is observed between the Ni stable isotope composition of the organic-rich sediments and TOC, suggesting that fractionation is not determined by changes in the organic carbon reservoir.~~

~~6. Similarly, there is no correlation between $\delta^{60}\text{Ni}$ and Ni abundance or bottom-water redox conditions, suggesting that the process of Ni uptake and enrichment at the sediment-water interface, and the degree of oxygenation in the water column do not exert primary control on isotopic fractionation.~~

~~7. Following evidence from Gall et al. (2013), it is probable the continental weathering process may induce isotopic fractionation.~~ The relatively heavy Ni stable

isotope composition of marine sediments may also in part reflect influxes of dissolved Ni from hydrothermal sources ($\delta^{60}\text{Ni} = 1.5$ ‰; Gall et al., 2013). However, further work is needed to investigate this.

The complexity of the sediment-seawater system may be the key factor that causes such enhanced levels of Ni isotope fractionation in marine sediments relative

to meteorites, basalts and continental sediments. This preliminary dataset has produced some new and important data that can be the basis for further research of Ni in organic-rich marine sediments. As such, it is recommended that the relationships between Ni isotope fractionation and factors ubiquitous to the marine depositional system, such as bottom-water redox conditions, the type of organic matter present, organic matter preservation and TOC, are further explored.

Figure captions

Figure 1: Map and photograph showing the location of the Sinemurian-Pliensbachian GSSP section, Robin Hood's Bay, UK.

Figure 2: Graphic log showing the Sinemurian-Pliensbachian boundary GSSP and the relative locations of the samples analysed in this study. Samples used for Ni isotope analysis are in bold. Bed number classification taken from Hesselbo and Jenkyns (1995).

Figure 3: Present-day maturity map of the Exshaw Formation within Alberta, Canada (modified from Creaney and Allan, 1991). Map shows the location of the thermally immature, mature and overmature zones parallel to the Rocky Mountain Front, and the location of the well from which the core samples used in this study originate.

Figure 4: Nickel isotope ($\delta^{60}\text{Ni}$), Ni abundance, and TOC profiles for the Sinemurian-Pliensbachian section, presented against a corresponding stratigraphic column and graphic log. Black dashed line indicates the position of the Sinemurian-Pliensbachian boundary. ¹Bed numbers are from Hesselbo and Jenkyns (1995).

Figure 5: Plot showing the relationship between TOC and $\text{V}/(\text{V}+\text{Ni})$ for the Pennsylvanian Stark Shale Member samples (solid black squares) detailed in Hatch and Leventhal (1992), Robin Hood's Bay sediments (hollow diamonds; this study) and the Exshaw Formation shales (hollow triangles; this study). Black dashed lines mark the parameters discussed in Hatch and Leventhal (1992), whereby values of > 2.5 wt. % TOC correspond to $\text{V}/(\text{V}+\text{Ni})$ values > 0.75 for the Pennsylvanian Stark Shale Member.

Figure 6: Nickel stable isotope data for organic-rich marine sediments from Robin Hood's Bay, UK (RHB) and the Exshaw Formation. The grey box represents the average of the Ni isotope data for meteorites, basalts and continental sediments (~ 0.2 ‰ and 1 standard deviation either side of this; Cameron et al., 2009). The white circles show Ni isotope data from ferromanganese crusts (taken from Gall et al., 2013).

Table 1: Previously established values for the trace element ratios and their corresponding depositional paleoredox conditions.

Table 2: Summary of trace element and TOC data and the associated ratios used for paleoredox proxies, for the Robin Hood's Bay and Exshaw Formation marine sediments.

Table 3: New nickel stable isotope data for a selection of Robin Hood's Bay and Exshaw Formation marine sediments.

Table 4: A summary of elemental data for average shale, average upper continental crust, Robin Hood's Bay and Exshaw Formation marine sediments.

References

- Alberdi, M., and Lafargue, E., 1993, Vertical variations of organic matter content in Guayuta Group (upper Cretaceous), Interior Mountain Belt, Eastern Venezuela: *Organic Geochemistry*, v. 20, no. 4, p. 425-436.
- Birck, J. L., and Lugmair, G. W., 1988, Nickel and chromium isotopes in Allende inclusions: *Earth and Planetary Science Letters*, v. 90, no. 2, p. 131-143.
- [Brennecka, G. A., Wasylenki, L. E., Bargar, J. R., Weyer, S., and Anbar, A. D., 2011, Uranium Isotope Fractionation during Adsorption to Mn-Oxyhydroxides: *Environmental Science and Technology*, v. 45, no. 4, p. 1370-1375.](#)
- Cameron, V., Vance, D., Archer, C., and House, C. H., 2007, Nickel stable isotopes as biogeochemical tracers, *Goldschmidt Conference Abstracts*, p. A141.
- Cameron, V., Vance, D., Archer, C., and House, C. H., 2009, A biomarker based on the stable isotopes of nickel: *Proceedings of the National Academy of Sciences*, v. 106, p. 10944-10948.
- Cameron, V., Vance, D., and Poulton, S., 2011, Nickel isotopes, BIFs and the Archean oceans, *Goldschmidt Conference Abstracts, Mineralogical Magazine*, p. 615.
- Cameron, V., House, C. H., and Brantley, S. L., 2012, A First Analysis of Metallome Biosignatures of Hyperthermophilic Archea: *Archea*, v. 2012, p. 1-12.
- Cameron, V., and Vance, D., 2014, Heavy nickel isotope compositions in rivers and the oceans, *Geochimica et Cosmochimica Acta*, v. 128, p. 195-211.
- Caplan, M. L., and Bustin, R. M., 1998, Sedimentology and sequence stratigraphy of Devonian-Carboniferous strata, southern Alberta: *Bulletin of Canadian Petroleum Geology*, v. 46, p. 487-514.

676 Caplan, M. L., and Bustin, R. M., 1999, Palaeoceanographic controls on geochemical
677 characteristics of organic-rich Exshaw mudrocks: role of enhanced primary
678 production: *Organic Geochemistry*, v. 30, no. 2-3, p. 161-188.

679 Chen, J. H., Papanastassiou, D. A., and Wasserburg, G. J., 2009, A search for nickel
680 isotopic anomalies in iron meteorites and chondrites: *Geochimica et*
681 *Cosmochimica Acta*, v. 73, no. 5, p. 1461-1471.

682 Cook, D. L., Wadhwa, M., Clayton, R., Dauphas, N., Janney, P. E., and Davis, A. M.,
683 2007, Mass-dependent fractionation of nickel isotopes in meteoritic metal:
684 *Meteoritics and Planetary Science*, v. 42, no. 12, p. 2067-2077.

685 Creaney, S., and Allan, J., 1991, Hydrocarbon generation and migration in the
686 Western Canada sedimentary basin: Geological Society, London, Special
687 Publications, v. 50, no. 1, p. 189-202.

688 Creaser, R. A., Sannigrahi, P., Chacko, T., and Selby, D., 2002, Further evaluation of
689 the Re-Os geochronometer in organic-rich sedimentary rocks: a test of
690 hydrocarbon maturation effects in the Exshaw Formation, Western Canada
691 Sedimentary Basin: *Geochimica et Cosmochimica Acta*, v. 66, no. 19, p. 3441-
692 3452.

693 [Cumming, V. M., Selby, D., and Lillis, P., 2012, Re-Os geochronology of the lacustrine](#)
694 [Green River Formation: Insights into direct depositional dating of lacustrine](#)
695 [successions, Re-Os systematics and paleocontinental weathering: *Earth and*](#)
696 [*Planetary Science Letters*, v. 359-360, p. 194-205.](#)

697 Dean, W. T., Donovan, D. T., and Howarth, M. K., 1961, The Liassic ammonite Zones
698 and Subzones of the North West European Province: *Bulletin of the Natural*
699 *History Museum*, v. 4, p. 435-505.

700 Dera, G., Pucéat, E., Pellenard, P., Neige, P., Delsate, D., Joachimski, M. M., Reisberg,
701 L., and Martinez, M., 2009, Water mass exchange and variations in seawater
702 temperature in the NW Tethys during the Early Jurassic: Evidence from
703 neodymium and oxygen isotopes of fish teeth and belemnites: Earth and
704 Planetary Science Letters, v. 286, no. 1-2, p. 198-207.

705 Dewaker, K. N., Chandra, K., Arunachalam, J., and Karunasagar, D., 2000, Isotopic
706 fractionation of Ni60/Ni61 in kerogen and bitumen samples: Current Science,
707 v. 79, no. 12, p. 1720-1723.

708 Dill, H., 1986, Metallogensis of early Paleozoic graptolite shales from the
709 Graefenthal Horst (Northern Bavaria-Federal Republic of Germany):
710 Economic Geology, v. 81, p. 889-903.

711 Ellrich, J., Hirner, A., and Stärk, H., 1985, Distribution of trace elements in crude oils
712 from southern Germany: Chemical Geology, v. 48, no. 1-4, p. 313-323.

713 Frausto da Silva, J.J.R., and Williams, R.J.P., 2001, The Biological Chemistry of the
714 Elements: The Inorganic Chemistry of Life, Oxford University Press, Oxford, p.
715 436-449.

716 Gall, L., Williams, H., Siebert, C., and Halliday, A., 2012, Determination of mass-
717 dependent variations in nickel isotope compositions using double spiking and
718 MC-ICPMS: Journal of Analytical Atomic Spectrometry, v. 27, no. 1, p. 137-
719 145.

720 Gall, L., Williams, H. W., Siebert, C., Halliday, A. N., Herrington, R. J., and Hein, J. R.,
721 2013, Nickel isotopic compositions of ferromanganese crusts and the
722 constancy of deep ocean inputs and continental weathering effects over the
723 Cenozoic: Earth and Planetary Science Letters, v. 375, p. 148-155.

724 Gradstein, F. M., Ogg, J. G., Schmitz, M. D., and Ogg, G. M. 2012. The Geologic Time
 725 Scale 2012. Elsevier.

726 [Harris, N. B., Mnich, C. A., Selby, D., and Korn, D., 2013, Minor and trace element and](#)
 727 [Re-Os chemistry of the Upper Devonian Woodford Shale, Permian Basin,](#)
 728 [west Texas: Insights into metal abundance and basin processes: Chemical](#)
 729 [Geology, v. 356, p. 76-93.](#)

730 Hatch, J. R., and Leventhal, J. S., 1992, Relationship between inferred redox potential
 731 of the depositional environment and geochemistry of the Upper
 732 Pennsylvanian (Missourian) Stark Shale Member of the Dennis Limestone,
 733 Wabaunsee County, Kansas, U.S.A: Chemical Geology, v. 99, no. 1-3, p. 65-82.

734 Herzog, G. F., Hall, G. S., and Brownlee, D. E., 1994, Mass fractionation of nickel
 735 isotopes in metallic cosmic spheres: Geochimica et Cosmochimica Acta, v. 58,
 736 no. 23, p. 5319-5323.

737 Hesselbo, S. P., and Jenkyns, H. C., 1995, A comparison of the Hettangian to Bajocian
 738 successions of Dorset and Yorkshire, in Taylor, P. D., ed., Field Geology of the
 739 British Jurassic, Geological Society, London, p. 105-150.

740 Hesselbo, S. P., Meister, C., and Grocke, D. R., 2000, A potential global stratotype for
 741 the Sinemurian-Pliensbachian boundary (Lower Jurassic), Robin Hood's Bay,
 742 UK: ammonite faunas and isotope stratigraphy: Geological Magazine, v. 137,
 743 no. 6, p. 601-607.

744 Jones, B., and Manning, D. A. C., 1994, Comparison of geochemical indices used for
 745 the interpretation of palaeoredox conditions in ancient mudstones: Chemical
 746 Geology, v. 111, no. 1-4, p. 111-129.

747 Jones, C. E., Jenkyns, H. C., and Hesselbo, S. P., 1994, Strontium isotopes in Early
 748 Jurassic seawater: *Geochimica et Cosmochimica Acta*, v. 58, no. 4, p. 1285-
 749 1301.

750 Kohman, T. P., and Robison, M. S., 1980, Iron-60 as a possible heat source and
 751 chronometer in the early solar system: *Lunar and Planetary Science*, v. 11, p.
 752 564-566.

753 [Konhauser, K. O., Pecoits, E., Lalonde, S. V., Papineau, D., Nisbet, E. G., Barley, M. E.,](#)
 754 [Arndt, N. T., Zahnle, K., and Kamber, B. S., 2009, Oceanic nickel depletion and](#)
 755 [a methanogen famine before the Great Oxidation Event: *Nature*, v. 458, p.](#)
 756 [750-753.](#)

757 Leenheer, M. J., 1984, Mississippian Bakken and other equivalent formations as
 758 source rocks in the Western Canada basin: *Organic Geochemistry*, v. 6, p.
 759 521-533.

760 Lewan, M. D., 1984, Factors controlling the proportionality of vanadium to nickel in
 761 crude oils: *Geochimica et Cosmochimica Acta*, v. 48, no. 11, p. 2231-2238.

762 Lewan, M. D., and Maynard, J. B., 1982, Factors controlling enrichment of vanadium
 763 and nickel in the bitumen of organic sedimentary rocks: *Geochimica et*
 764 *Cosmochimica Acta*, v. 46, no. 12, p. 2547-2560.

765 Li, H.-Y., Schoonmaker, J., 2003, Chemical composition and mineralogy of marine
 766 sediments. In: *Treatise on Geochemistry. Sediments, Diagenesis, and*
 767 *Sedimentary Rocks*, v. 7, p. 1-35.

768 López, L., Lo Mónaco, S., Galarraga, F., Lira, A., and Cruz, C., 1995, VNi ratio in
 769 maltene and asphaltene fractions of crude oils from the west Venezuelan
 770 basin: correlation studies: *Chemical Geology*, v. 119, no. 1-4, p. 255-262.

771 Manning, L. K., Frost, C. D., and Branthaver, J. F., 1991, A neodymium isotopic study
 772 of crude oils and source rocks: potential applications for petroleum
 773 exploration: *Chemical Geology*, v. 91, no. 2, p. 125-138.

774 Meijer, N. C., Johnston, D. I., and Fullmer, E. G., 1994, Devonian stratigraphy and
 775 depositional history across Peace River Highland, west central Alberta and
 776 nearby British Columbia: *Geological Survey of Canada Open File 2851*, p. 40
 777 pp.

778 Meister, C., Aberhan, M., Blau, J., Dommergues, J.-L., Feist-Burkhardt, S., Hailwood,
 779 E. A., Hart, M., Hesselbo, S. P., Hounslow, M. W., Hylton, M., Morton, N.,
 780 Page, K., and Price, G. D., 2006, The Global Boundary Stratotype Section and
 781 Point (GSSP) for the base of the Pliensbachian Stage (Lower Jurassic), Wine
 782 Haven, Yorkshire, UK: *Episodes*, v. 29, no. 2, p. 93-114.

783 Morand, P., and Allègre, C. J., 1983, Nickel isotopic studies in meteorites: *Earth and*
 784 *Planetary Science Letters*, v. 63, no. 2, p. 167-176.

785 Moynier, F., Blichert-Toft, J., Telouk, P., Luck, J.-M., and Albarède, F., 2007,
 786 Comparative stable isotope geochemistry of Ni, Cu, Zn, and Fe in chondrites
 787 and iron meteorites: *Geochimica et Cosmochimica Acta*, v. 71, no. 17, p.
 788 4365-4379.

789 Ottley, C. J., Pearson, D. G., and Irvine, G. J., 2003, A routine method for the
 790 dissolution of geological samples for the analysis of REE and trace elements
 791 via ICP-MS, *in* Holland, G., and Tanner, S. D., eds., *Plasma source mass*
 792 *spectrometry: applications and emerging technologies*, p. 221-230.

793 Palmer, M. R., Kenison Falkner, K., Turekian, K. K., and Calvert, S. E., 1988, Sources of
 794 osmium isotopes in manganese nodules: *Geochimica et Cosmochimica Acta*,
 795 v. 52, no. 5, p. 1197-1202.

796 Peucker-Ehrenbrink, B., and Hannigan, R. E., 2000, Effects of black shale weathering
 797 on the mobility of rhenium and platinum group elements: *Geology*, v. 28, no.
 798 5, p. 475-478.

799 Piggott, N., and Lines, M. D., 1992, A case study of migration from the West Canada
 800 Basin, *in* England, W. A., and Fleet, A. J., eds., *Petroleum Migration*, Volume
 801 59, Geological Society Special Publication, p. 207-225.

802 Powell, J. H., 1984, Lithostratigraphical nomenclature of the Lias Group in the
 803 Yorkshire Basin: *Proceedings of the Yorkshire Geological Society*, v. 45, p. 51-
 804 57.

805 Quitté, G., Meier, M., Latkoczy, C., Halliday, A.N., and Günther, D., 2006, Nickel
 806 isotopes in iron meteorites—nucleosynthetic anomalies in sulphides with no
 807 effects in metals and no trace of ^{60}Fe : *Earth and Planetary Science Letters*, v.
 808 242, p. 16-25.

809 Quitté, G., and Oberli, F., 2006, Quantitative extraction and high precision isotope
 810 measurements of nickel by MC-ICPMS: *Journal of Analytical Atomic*
 811 *Spectrometry*, v. 21, p. 1249-1255.

812 Richards, B. C., and Higgins, A. C., 1988, Devonian-Carboniferous beds of the Palliser
 813 and Exshaw formations at Jura Creekm Rocky Mountains, southwestern
 814 Alberta, *in* McMillan, N. J., ed., *Devonian of the world*, Canadian Society of
 815 *Petroleum Geologists Memoir*, Volume 14, p. 399-412.

816 Richards, B. C., Mamet, B. L., and Bamber, E. W., 1999, Uppermost Devonian and
817 Carboniferous sequence stratigraphy, biostratigraphy and basin
818 development, Banff region, southwestern Alberta, XIV International Congress
819 on the Carboniferous and Permian, Field Trip, 4-7 and 4-17 Guidebook:
820 Calgary, Alberta.

821 Richards, C., Ross, G. M., and Utting, J., 2002, U-Pb geochronology, lithostratigraphy
822 and biostratigraphy of tuff in the Upper Famennian to Tournaisian Exshaw
823 Formation: Evidence for a mid-Paleozoic magmatic arc on the northwestern
824 margin of North America, *in* Hills, L. V., Henderson, C. M., and Bamber, E. W.,
825 eds., Carboniferous and Permian of the World: XIV ICCP Proceedings, Volume
826 19, Can Soc Petrol Geol Mem, p. 158-207.

827 Rimmer, S. M., 2004, Geochemical paleoredox indicators in Devonian-Mississippian
828 black shales, Central Appalachian Basin (USA), *Chemical Geology*, v. 206, no.
829 3-4, p. 373-391.

830 [Rudnick, R. L., and Gao, S., 2003, 3.01 Composition of the Continental Crust: Treatise](#)
831 [on Geochemistry, v. 3, p. 1-64.](#)

832 Schovsbo, N. H., 2001, Why barren intervals? A taphonomic case study of the
833 Scandinavian Alum Shale and its faunas: *Lethaia*, v. 34, no. 4, p. 271-285.

834 Sclater, F., Boyle, E., Edmond, J., 1976, On the marine geochemistry of nickel: *Earth*
835 *and Planetary Science Letters*, v. 31, p. 119-128.

836 Selby, D., and Creaser, R. A., 2005, Direct radiometric dating of the Devonian-
837 Mississippian time-scale boundary using the Re-Os black shale
838 geochronometer: *Geology*, v. 33, p. 545-548.

839 Selby, D., Mutterlose, J., and Condon, D. J., 2009, U-Pb and Re-Os geochronology of
840 the Aptian/Albian and Cenomanian/Turonian stage boundaries: Implications
841 for timescale calibration, osmium isotope seawater composition and Re-Os
842 systematics in organic-rich sediments: *Chemical Geology*, v. 265, no. 3-4, p.
843 394-409.

844 Sellwood, B. W., and Jenkyns, H. C., 1975, Basins and swells and the evolution of an
845 epeiric sea (Pliensbachian-Bajocian of Great Britain): *Journal of the Geological*
846 *Society*, v. 131, no. 4, p. 373-388.

847 Shimamura, T., and Lugmair, G. W., 1983, Ni isotopic compositions in Allende and
848 other meteorites: *Earth and Planetary Science Letters*, v. 63, no. 2, p. 177-
849 188.

850 Spath, L. F., 1923, Correlation of the Ibex and Jamesoni Zones of the Lower Lias:
851 *Geological Magazine*, v. 60, p. 6-11.

852 Wasylenki, L., Spivak-Birndorf, L., Howe, H., and Wells, R., 2014, Experiments reveal
853 the mechanism by which Ni isotopes fractionate in the weathering
854 environment: *Goldschmidt Abstracts*, 2661.

855 Wasylenki, L. E., Rolfe, B. A., Weeks, C. L., Spiro, T. G., and Anbar, A. D., 2008,
856 Experimental investigation of the effects of temperature and ionic strength
857 on Mo isotope fractionation during adsorption to manganese oxides:
858 *Geochimica et Cosmochimica Acta*, v. 72, p. 5997-6005.

859 Wasylenki, L. E., Weeks, C. L., Bargar, J. R., Spiro, T. G., Hein, J. R., and Anbar, A. D.,
860 2011, The molecular mechanism of Mo isotope fractionation during
861 adsorption to birnessite: *Geochimica et Cosmochimica Acta*, v. 75, no. 17, p.
862 5019-5031.

863 | Wedepohl, K. H., 1971, Environmental influences on the chemical composition of
864 | shales and clays: Physics and Chemistry of the Earth, v. 8, p. 305-333.
865 | Xue, S., Herzog, G. F., Hall, G. S., Klein, J., Middleton, R., and Juenemann, D., 1995,
866 | Stable nickel isotopes and cosmogenic beryllium-10 and aluminum-26 in
867 | metallic spheroids from Meteor Crater, Arizona: Meteoritics, v. 30, p. 303-
868 | 310.

Characterising the nickel isotopic composition of organic-rich marine sediments

Highlights

- New Ni stable isotope data for two suites of organic-rich marine sediments (ORMS)
- The Ni isotope compositions (Ni IC) of both suites are comparable
- The Ni IC of ORMS are heavier than bulk Earth samples and present-day seawater
- The Ni IC of ORMS are comparable to that of ferromanganese crusts
- Factors ubiquitous to the marine realm are likely to drive fractionation in ORMS

Characterising the nickel isotopic composition of organic-rich marine sediments

Sarah J. Porter^{1,2*}, David Selby¹, and Vyllinniskii Cameron³

¹ Department of Earth Sciences, Science Labs, Durham University, Durham, DH1 3LE, UK

² Chemostrat Ltd., Unit 1 Ravenscroft Court, Buttington Cross Enterprise Park, Welshpool, Powys, SY21 8SL, UK

³ Bristol Isotope Group, School of Earth Sciences, University of Bristol, Bristol BS8 1RJ, UK

*Corresponding author: Sarah J. Porter. Email: sarahporter@chemostrat.com;

Tel.: +44(7889)838599

Keywords: Nickel isotope fractionation, Ni isotopes, $\delta^{60}\text{Ni}$, organic-rich marine sediments, Sinemurian-Pliensbachian GSSP, Exshaw Formation, redox

Abstract

New Ni stable isotope data ($\delta^{60}\text{Ni}$) determined by double-spike MC-ICP-MS for two geologically distinct suites of organic-rich marine sediments from the Sinemurian-Pliensbachian (S-P) Global Stratotype Section and Point (GSSP; Robin Hood's Bay, UK) and the Devonian-Mississippian Exshaw Formation (West Canada Sedimentary Basin) is presented herein. These sediments yield $\delta^{60}\text{Ni}$ values of between 0.2 ‰ and 2.5 ‰, and predominantly have Ni isotopic compositions that are heavier than those of abiotic terrestrial and extraterrestrial samples (0.15 ‰ and 0.27 ‰), and in some cases present-day seawater (1.44 ‰) and dissolved Ni from riverine input (0.80 ‰). In addition, the observed degree of isotopic fractionation in the marine sediments is far greater than that of these other sample matrices. However, a strong similarity is exhibited between the $\delta^{60}\text{Ni}$ values of the organic-rich sediments studied here and those of ferromanganese crusts (0.9 to 2.5 ‰), suggesting that factors ubiquitous to

the marine environment are likely to play a key role in the heightened level of isotopic fractionation in these sample matrices.

A lack of correlation between the Ni stable isotope compositions of the organic-rich sediments and Ni abundance, suggests that isotopic fractionation in these sediments is not controlled by incorporation or enrichment of Ni during sediment accumulation. Further, no relationship is observed between $\delta^{60}\text{Ni}$ and TOC concentrations or bottom-water redox conditions, indicating that the organic carbon reservoir and levels of oxygenation at the sediment-water interface do not exert a primary control on Ni isotope fractionation in marine sediments. Following examination of these relationships, it is therefore more likely that the heavy Ni isotope compositions of marine sediments are controlled by the weathering environment and the dominant sources of dissolved Ni into the global ocean reservoir.

57

58 **1. Introduction**

59

60 For several decades previous investigations of Ni isotopes have focused
61 predominantly on characterising radiogenic isotopic fractionation in extraterrestrial
62 materials, with a view to enhancing our understanding of planetary processes and
63 the isotopic composition of the early Solar System (eg. Kohman and Robison, 1980;
64 Morand and Allègre, 1983; Shimamura and Lugmair, 1983; Birck and Lugmair, 1988;
65 Herzog et al., 1994; Xue et al., 1995; Quitté et al., 2006; Cook et al., 2007; Moynier et
66 al., 2007; Chen et al., 2009). Further, the role of Ni as a bioessential trace metal (eg.
67 Frausto da Silva and Williams, 2001; Cameron et al., 2007; 2009) has led to the
68 recognition that the stable isotopes of Ni may have the potential to be utilised as a
69 powerful biological tool for studies of early life on Earth (Cameron et al., 2009;
70 2012).

71 In addition to its role in cosmochemical and biochemical investigations, the
72 potential of Ni to significantly enhance our understanding of organic-rich
73 sedimentary environments and to provide a powerful geological tracer in the
74 petroleum realm has been recognised, following pioneering work by Lewan and
75 Maynard (1982) and Lewan (1984) (eg. Ellrich et al., 1985; Manning et al., 1991;
76 Alberdi and Lafargue, 1993; López et al., 1995). However, these studies focused on
77 the elemental distribution of Ni rather than on its isotopic characterisation, and as
78 such, no study currently exists that evaluates the behaviour of Ni stable isotopes in
79 organic-rich sediments or indeed within a stratigraphic profile. This can be attributed
80 to Ni being a relatively newly investigated system, together with the difficulty

81 associated with purifying Ni from such complex sample matrices, that has only
82 recently been overcome through advancements in analytical and mass spectrometry
83 techniques (eg. Gall et al., 2012; Cameron and Vance, 2014).

84 Until now, Ni stable isotope systematics in organic-rich sedimentary matrices
85 have not been investigated. Indeed, it is only recently that the Ni isotopic
86 composition of seawater and the sources of Ni to the global oceanic reservoir have
87 been determined (e.g. Cameron and Vance, 2014; Gall et al., 2013). Present-day
88 seawater has an average $\delta^{60}\text{Ni}$ value of 1.44 ± 0.15 ‰, with apparent global isotopic
89 homogeneity (Cameron and Vance, 2014). The oceanic residence time of Ni has been
90 calculated as ~30 kyr (Cameron and Vance, 2014), which is significantly longer than
91 the mixing time of the global oceans (~2,000 yrs; Palmer et al., 1988). This would be
92 sufficient for the ocean to have an isotopically homogenous Ni composition.
93 Cameron et al. (2014) also demonstrate that draw-down of Ni from the surface to
94 deep ocean during trace metal cycling is not accompanied by isotopic fractionation,
95 thus further suggesting that the modern ocean is isotopically homogenous. In the
96 absence of any Ni isotope studies on banded iron formation and shale datasets, it is
97 difficult to speculate on processes occurring in an ancient ocean. However,
98 examination of Ni/Fe data from banded iron formations and extrapolated maximum
99 dissolved Ni concentration values in sea water through time (Konhauser et al., 2009),
100 demonstrates that dissolved nickel concentrations may have reached present day
101 values by ~550 Ma. As such, given the age of the sediments being studied herein
102 (~190-360 Ma), it is appropriate to use what we know regarding modern ocean
103 circulation and fractionation processes to hypothesise about processes acting in the
104 ancient oceans. The predominant input of dissolved Ni to the oceans occurs via

riverine influx, which has been suggested to yield an annual discharge- and concentration-weighted $\delta^{60}\text{Ni}$ average of +0.80 ‰ (Cameron and Vance, 2014). Significant variability in the riverine isotopic composition has been observed (+0.29 to +1.34 ‰), which has been attributed to isotopic fractionation of Ni during weathering of continental crust, resulting in heavier $\delta^{60}\text{Ni}$ values in rivers and seawater. In addition, mineral dust and volcanic ash also contribute to the oceanic Ni budget (Li and Schoonmaker, 2003), as well as hydrothermal vent fluids ($\delta^{60}\text{Ni} = 1.5$ ‰; Gall et al., 2012).

Herein we present the first attempt at creating a Ni isotope stratigraphic profile for an organic-rich sedimentary succession. The marine section across the Sinemurian-Pliensbachian Global Stratotype Section and Point (GSSP), Robin Hood's Bay, UK, is ideally suited to the present study, as it well understood biostratigraphically (Hesselbo et al., 2000; Meister et al., 2006) and has been previously characterised using other isotope stratigraphy techniques, including strontium ($^{87}\text{Sr}/^{86}\text{Sr}$; Jones et al., 1994; Hesselbo et al., 2000), oxygen ($\delta^{18}\text{O}$), carbon ($\delta^{13}\text{C}$) (Hesselbo et al., 2000), and Re-Os isotopes (Porter et al., 2013). The section is also consistently thermally immature (the rocks have not been subjected to enough heat or pressure to convert any kerogens present to hydrocarbons), thereby eliminating any potential effects of thermal maturation on the Ni isotope signature. In addition, to draw comparison between the isotopic composition of samples of different depositional ages and environments, we present Ni isotope data from a selection of thermally immature black shale samples from a core of the Exshaw Formation, Canada.

To accurately assess and interpret any stratigraphic variation of Ni isotopes in the Robin Hood's Bay section and Exshaw Formation samples, it is critical to determine whether any fluctuations in paleoredox conditions occur. Nickel primarily occupies one oxidation state in the natural environment (Ni^{2+}), suggesting that it is not redox sensitive. However, its preferential association with redox-sensitive metallo-organic complexes (porphyrins) in organic-rich sediments (Lewan and Maynard, 1982) indicates that certainly within these sample matrices, redox conditions at the time of sediment deposition may directly impact the degree of enrichment or depletion of Ni. Herein, paleoredox conditions have been established for the Sinemurian-Pliensbachian GSSP section and the Exshaw Formation sample suite. Although one previous study (Dewaker et al., 2000) provides a preliminary dataset for the Ni isotope composition of sediments from 3 different basins, our understanding of the behaviour of Ni isotope systematics within organic-rich sediments is currently non-existent. Further, advancements in analytical techniques over the past decade suggest that the methodology employed by Dewaker et al. (2000) may not have been optimal for Ni separation or Ni stable isotope analysis.

This paper presents the first detailed study of nickel stable isotope systematics in organic-rich marine sediments. Analysis of marine sediments of different depositional ages and from two geologically distinct settings, the Sinemurian-Pliensbachian boundary (UK) and the Devonian-Mississippian Exshaw Formation (Canada), yields comparable Ni isotope compositional values for both sites. These samples provide insight into the incorporation of Ni into ocean sediments, and allow evaluation of the contribution of the various dissolved Ni fluxes to the seawater during these time periods.

2. Geological Setting

2.1 The Sinemurian-Pliensbachian boundary GSSP, Robin Hood's Bay, UK

The Sinemurian-Pliensbachian boundary, established from the succession's complete ammonite assemblages (Spath, 1923; Dean et al., 1961; Hesselbo et al., 2000; Meister et al., 2006), occurs in the Pyritous Shales of the Redcar Mudstone Formation within the Lias Group at Robin Hood's Bay (Powell, 1984; Fig. 1). At this point in the Early Jurassic, Robin Hood's Bay was positioned on the margins of a shallow epicontinental sea (eg. Dera et al., 2009) that covered most of Northern Europe, including Britain, during the Mesozoic (Sellwood and Jenkyns, 1975). The facies changes across the boundary, from pale siliceous to finer, more organic-rich mudstones (Fig. 2), indicate an overall relative increase in sea level of at least regional extent (eg. Hesselbo et al., 2000; Meister et al., 2006; Porter et al., 2013).

The age for the base of the Pliensbachian has been defined by the Geological Time Scale (GTS) 2012 as 189.6 ± 1.5 Ma (Gradstein et al., 2012), derived from cycle-scaled linear Sr trends and ammonite occurrences (as noted above; also includes the lowest occurrence of *Bifericeras donovani*; Gradstein et al., 2012).

2.2 Exshaw Formation, West Canada Sedimentary Basin (WCSB)

The West Canada Sedimentary Basin (WCSB) trends approximately NW-SE between the Canadian Shield to the East and the Western Cordillera to the West

(Piggott and Lines, 1992). Within the WCSB lies the Exshaw Formation, a thin but laterally continuous unit (2-12 m thick; Leenheer, 1984; Creaney and Allan, 1991). The Exshaw Formation in south-west and western Alberta (Fig. 3) comprises a lower member of organic-rich mudrocks and black shales which rest with minor disconformity upon Upper Devonian carbonate strata (Richards et al., 1999), and are abruptly to gradationally overlain by bioturbated shelf siltstones (Caplan and Bustin, 1998, 1999; Creaser et al., 2002). The depositional interval of the lower black shale unit is well constrained biostratigraphically; between the *expansa* and *duplicata* zones of Late Famennian to Early Tournaisian time (over a maximum time period of ~363 – 360 Ma; Caplan and Bustin, 1998). These lower black shales are dark grey, bituminous, relatively thin (consistently between 3-5 m; Meijer et al., 1994) and widespread (Meijer et al., 1994). The Devonian-Mississippian boundary (Exshaw-type section at Jura Creek, ~80 km west of Calgary, Alberta, Canada) represents the boundary between the upper calcareous and lower non-calcareous black shale units (Richards and Higgins, 1988). Selby and Creaser (2005) provide an absolute Model 1 Re-Os age for this boundary, and thus the top of the lower black shale unit, of 361.3 ± 2.4 Ma. In addition, U-Pb monazite data from a tuff horizon close to the base of the lower black shale member constrains an absolute depositional age for this unit of 363.4 ± 0.4 Ma (Richards et al., 2002). Deposition at this time represents part of a continent-wide Famennian-Tournaisian black shale event, and in turn, a possible ocean anoxic event (Piggott and Lines, 1992).

3. Sampling

200

201 A set of 32 samples (SP7-09 to SP39-09) was collected from the Pyritous
202 Shales Member of the Redcar Mudstone Formation, along a 6 m vertical section
203 bracketing the Sinemurian–Pliensbachian boundary (sample SP22-09) at Robin
204 Hood’s Bay (Fig. 2). This marine sequence contains a rich fauna of ammonites both
205 above and below the boundary interval (Hesselbo et al., 2000). Total organic carbon
206 analysis was conducted on all samples, with a consistent sampling interval of ~20 cm
207 for 3 m above and 3 m below the boundary from Beds 69–75 (except within Bed 72,
208 where a smaller sampling interval of ~15 cm was used). Of these samples, 14 were
209 analysed for Ni isotopes at a sampling interval of ~40 cm (Fig. 2).

210 Four samples from the Lower member of the Exshaw Formation were
211 collected from the Alberta Energy and Utilities Board, Core Research Centre, Calgary
212 (Fig. 3). The samples were taken from core 3-19-80-23W5, as detailed in Piggot and
213 Lines (1992) and Creaser et al. (2002). All samples are thermally immature, fine-
214 grained black shales containing very thin parallel and undulating laminations, and
215 showing no evidence of post-depositional disturbance. Drill core samples were
216 obtained to avoid any potential effects of surface weathering, including loss of
217 organic matter (PeuckerEhrenbrink and Hannigan, 2000). Further, edges of the core
218 were polished and where possible samples were taken from the central part of the
219 core.

220

221

222 **4. Analytical Protocol**

223

224 4.1 Trace element abundance and TOC

225 The elements V, Cr, Ni and Co were analysed in this study in order to look at relative
226 changes of depositional redox conditions in the sediments of interest. Samples were
227 prepared for trace element analysis at the Durham Geochemistry Group (University
228 of Durham, UK) following the method of Ottley et al., (2003). Sample powders (~100
229 mg) were digested in a 4:1 solution of 29 N HF and 16 N HNO₃ at ~150 °C for 48 hrs.
230 Samples were then evaporated to near rather than total dryness, to avoid
231 stabilisation of insoluble fluorides (Ottley et al., 2003). This was followed by the
232 addition of 1 ml 16 N HNO₃ and evaporation to near dryness. The previous stage was
233 repeated before the addition of 2.5 ml 16 N HNO₃ and ~10 ml 18MΩ water to create
234 a ~4 N HNO₃ solution. Sample beakers were capped and heated on the hotplate
235 overnight at ~100 °C. Once cooled, 1 ml of 1 ppm internal Re and Rh spike was
236 added to the samples (to yield 20 ppb Re and Rh in the final analyte solution) before
237 dilution up to 50 ml with MQ, yielding a ~0.5 N HNO₃ solution. Prior to analysis,
238 samples were diluted 10-fold by taking 1 ml from the 50 ml solution and diluting it to
239 10 ml using 0.5 N HNO₃. Samples were then analysed using the Thermo X-Series
240 Quadrupole Inductively Coupled Plasma Mass Spectrometer (ICP-MS). Replicate
241 analyses of USGS International Reference Materials (RMs) AGV-1, BHVO-1 and W-2
242 were conducted for calibration per sample set.

243 Total organic carbon measurements were performed at Durham University
244 using a Costech Elemental Analyser (ECS 4010) coupled to a ThermoFinnigan Delta V
245 Advantage. Total organic carbon was obtained as part of the isotopic analysis
246 ($\delta^{13}\text{C}_{\text{org}}$) using an internal standard (Glutamic Acid, 40.82 % C). Data accuracy was
247 monitored through routine analyses of in-house standards, which are stringently

calibrated against international standards (eg. USGS 40, USGS 24, IAEA 600, IAEA CH6).

4.2 Nickel stable isotopes

All Ni isotope analyses were conducted at the University of Bristol. Samples (~100 mg) were digested in closed PFA Beakers (Savillex, Minnetonka, MN) in a mixture of concentrated HF and HNO₃ (3:1) at 140 °C for 48 hrs. Dried samples were treated further with 7 N HCl. Chemical separation, purification and analyses of Ni isotopes was carried out as described in detail in Cameron et al. (2009) and Cameron and Vance (2014). Briefly, sample aliquots were spiked and allowed to equilibrate under heating in closed vials overnight. This was followed by drying down and treatment with 7 N HCl + H₂O₂. The spiked samples were then put through a 3-stage column procedure that in turn removes Fe and Zn, separates Ni from the bulk sample matrix, and final purification to remove any residual Fe and Zn. The first ion-exchange column (AG MP-1M, Bio-Rad) is used to remove Fe and Zn. The dried samples are then taken up in 1M HCl/1 M ammonium citrate, and the pH adjusted to 8–9 before loading onto columns filled with Ni resin (Eichrom Technologies). This step separates Ni while removing all other matrix elements in the sample. After oxidation to remove Ni-bound DMG, the samples are finally put through a third column, which is a repeat of the first anion column, to clean up any residual Fe and Zn.

All analyses were conducted in low resolution mode using a ThermoFinnigan Neptune multi-collector (MC) ICP-MS coupled to an Aridus desolvating nebuliser system (CETAC, Omaha, NE, USA). Samples were introduced in 2% HNO₃ via a CPI

PFA nebuliser (50 µl/minute) and spray chamber. Prior to isotopic analysis, the $^{56}\text{Fe}/^{58}\text{Ni}$ ratio was manually checked in high resolution mode in all samples so that any potential isobaric interference from residual sample ^{58}Fe could be applied as a correction to Ni mass 58. Relative to the propagated internal uncertainty on $\delta^{60}\text{Ni}$, the correction was insignificant. Additionally, a small amount of N_2 was introduced to the Aridus sweep gas to reduce a potential interference from $^{40}\text{Ar}^{18}\text{O}$ at mass 58. To mitigate inaccuracies in the $\delta^{60}\text{Ni}$ brought on by any instrumental variations, measurements of the pure NIST SRM986 standard were made throughout the analytical session. The reproducibility and accuracy of all isotope ratios were monitored further by measurement of mixtures of the SRM986 standard with the double-spike. All isotopes were measured simultaneously in static mode using a multiple Faraday collector array. All Ni data are reported relative to NIST SRM986, in the standard delta notation ($\delta^{60}\text{Ni} = [({}^{60}\text{Ni}/{}^{58}\text{Ni})_{\text{sample}}/({}^{60}\text{Ni}/{}^{58}\text{Ni})_{\text{NISTSRM986}}]-1] \times 1000$), with all uncertainties reported to the 2σ level.

5. Results

5.1 Trace elements and TOC

The trace element ratios Ni/Co, V/Cr and V/(V+Ni) have been utilised by previous studies to evaluate paleoredox conditions at the time of sediment deposition (eg. Hatch and Leventhal, 1992; Jones and Manning, 1994; Schovsbo, 2001; Rimmer, 2004). Both Ni and V occur in highly stable tetrapyrrole complexes that are originally derived from chlorophyll and are preferentially preserved under anoxic conditions (Lewan and Maynard, 1982). When organic matter has been

extensively exposed to aerobic conditions, preservation of these tetrapyrrole complexes will be low and subsequently the organic matter will have low Ni and V contents. Chromium is not influenced by redox conditions, and thus because of its association with just the detrital fraction and not the organic matter (Dill, 1986), high V/Cr values (>2) are indicative of anoxic conditions. Both Ni and Co are found in pyrite (in addition to the occurrence of Ni in porphyrins), but high Ni/Co values are associated with anoxic conditions (Jones and Manning, 1994). The relationship between these ratios and depositional redox conditions are summarised in Table 1.

The abundances of Ni, Co, V, Cr and TOC for all samples from Robin Hood's Bay and the Exshaw Formation, are presented in Table 2. Both the Ni/Co and V/Cr indices for Robin Hood's Bay show that these sediments were deposited under predominantly oxic conditions. However, there is significant disagreement between these ratios and the $V/(V+Ni)$ index. Values for $V/(V+Ni)$ range from $\sim 0.51 - 0.89$ and indicate that anoxic conditions prevailed across the Sinemurian-Pliensbachian boundary. Further, six samples suggest that bottom-water circulation ceased and that conditions became euxinic intermittently between ~ 2.6 m above the boundary and ~ 1.9 m below it (Table 2).

The Ni/Co ratio in the Exshaw Formation sediments ranges from $13.8 - 21.4$, with all four samples falling within the suboxic-anoxic parameter (Table 2). Similarly, the $V/(V+Ni)$ ratio indicates that three of the samples were deposited under suboxic-anoxic conditions (SP8-10, SP10-10 and SP13-10; values of 0.67 , 0.69 and 0.67 , respectively). However, whilst V/Cr values of 7.2 and 9.0 suggest a suboxic-anoxic depositional environment for Exshaw Formation samples SP10-10 and SP13-10,

respectively, this ratio also yields values that are representative of dysoxic conditions for samples SP8-10 and SP9-10 (2.0 and 2.1, respectively).

Total organic carbon content is generally low in the Sinemurian-Pliensbachian sediments, varying from ~0.53 – 2.46 wt. % (Table 2; Fig. 4). The data shows only slight variation prior to the boundary (~0.57 – 0.86 wt. %; Fig. 4), but an overall gradual increase above the boundary (from ~0.58 – 2.46 wt. %; Fig. 4). Total organic carbon values in the Exshaw Formation samples range from 1.2 – 11 wt. %.

5.2 Nickel stable isotopes

New Ni stable isotope data for a select suite of the organic-rich sediments at Robin Hood's Bay is presented (see Table 3). From the base of Bed 71 the sampling interval for Ni isotope analysis is ~40 cm (Fig. 2). A profile of $\delta^{60}\text{Ni}$ values for the section is shown alongside Ni concentration and TOC for comparison (Fig. 4).

The $\delta^{60}\text{Ni}$ of these samples is extremely variable, ranging from 0.28 ± 0.05 – 1.60 ± 0.05 ‰ (Fig. 4; Table 3). Two noticeable peaks in $\delta^{60}\text{Ni}$ values are observed 0.8 m above and 2.1 m below the Sinemurian-Pliensbachian boundary (1.26 ± 0.05 ‰ and 1.60 ± 0.05 ‰, respectively) that approximately correlate with the tops of beds 70 and 74. The greatest range in $\delta^{60}\text{Ni}$ values occurs below the boundary (~1.32 ‰), compared to a range of ~0.97 ‰ above the boundary (Fig. 4). In this section and dataset there is no apparent relationship between the degree of Ni isotope fractionation and depositional redox conditions, TOC or stratigraphic height (Fig. 4).

Nickel stable isotope data for the Exshaw Formation is also presented in Table 3. The $\delta^{60}\text{Ni}$ values in these samples range from 0.46 ± 0.04 to 2.50 ± 0.04 ‰ (Table 3). As with the Robin Hood's Bay section, no relationship exists between $\delta^{60}\text{Ni}$

and sample depth or between $\delta^{60}\text{Ni}$ and depositional redox conditions, TOC or stratigraphic position (Fig. 4).

6. Discussion

6.1. Evaluating the suitability of $V/(V+Ni)$ as a redox proxy: How applicable is it?

The Ni/Co and V/Cr redox indices are recommended by a number of workers as the most reliable of the paleo-environmental proxies (eg. Jones and Manning, 1994; Rimmer, 2004), and have been used by several studies to provide accurate and consistent evaluations of paleoredox conditions at the time of sediment deposition (eg. Rimmer, 2004; Selby et al., 2009; this study). However, this study finds that there is significant disagreement between these indices and the $V/(V+Ni)$ index. For Robin Hood's Bay, the latter index suggests that the sediments were deposited in predominantly suboxic-anoxic bottom-waters, with intermittent euxinic periods. However, both the V/Cr and Ni/Co ratios indicate that the Robin Hood's Bay samples were deposited under largely oxic condition. Such disparity between the redox indices is also noted by both Rimmer (2004) and Selby et al. (2009), who observe that the $V/(V+Ni)$ index suggests suboxic-anoxic conditions for sediments otherwise indicated to have been deposited under oxic conditions by the V/Cr and Ni/Co ratios.

Preliminary work by Lewan and Maynard (1982) and Lewan (1984) suggested that redox potential was a dominant control on the wide range of $V/(V+Ni)$ values observed in petroleum source rocks and oils. Following this, Hatch and Leventhal

(1992) were the first to develop and utilise the $V/(V+Ni)$ index as a measure of relative redox potential in organic-rich sediments. Their study focused on applying this index specifically to marine black shales in the Pennsylvanian Stark Shale Member of the Dennis Limestone, Wabaunsee County, Kansas, USA (Hatch and Leventhal, 1992). Therefore, the ranges they defined for the $V/(V+Ni)$ ratio and the associated redox conditions (summarised in Table 1), are applicable to this specific geological basin and are sensitive to localised geochemical variations therein.

Hatch and Leventhal (1992) show that for the Stark Shale Member, with the exception of two outliers, low TOC values (<2.5 wt. %) correspond to $V/(V+Ni)$ values <0.75 , and samples containing greater TOC (>7.5 wt. %) have corresponding higher $V/(V+Ni)$ values (0.75; Fig. 5). However, this relationship is not observed in the majority of the Sinemurian-Pliensbachian or Exshaw Formation sediments, with samples containing low TOC providing a range in $V/(V+Ni)$ data from $\sim 0.33 - 0.89$. This immediately indicates that there are significant geochemical differences between these three geological sites. This may be due to differences in both geological age and stratigraphy, with the Stark Shale Member (Late Carboniferous) being a darker grey, non-sandy shale with higher TOC content (Hatch and Leventhal, 1992). As such, this comparison suggests that the redox index $V/(V+Ni)$, originally developed for a specific geological basin, may not be applicable to other geological sites, particularly those that possess differing geological and geochemical characteristics. Factors that may have a profound effect upon the applicability of such a threshold from one study to another include: differences in the influx of nutrients and trace elements, type and relative amounts of organic matter, and degrees of oceanic mixing (eg. Rimmer, 2004). However, these are preliminary

findings from a small dataset and further investigation is recommended. In agreement with Rimmer (2004), this study therefore suggests that caution should be taken when applying redox indices established by other studies for single geological sites.

6.2. Nickel stable isotope fractionation in marine sediments

Nickel stable isotope data for the Exshaw Formation and the Sinemurian-Pliensbachian GSSP is presented in Table 3 and Figure 6, and is the first to be obtained for a suite of organic-rich marine sediments. The Exshaw Formation shales define a realm of $\delta^{60}\text{Ni}$ values of 0.46 ± 0.04 to 2.50 ± 0.04 ‰ (a range of ~ 2.04 ‰; Fig. 6). This range overlaps with, and is comparable to the $\delta^{60}\text{Ni}$ data for the Sinemurian-Pliensbachian boundary GSSP (0.28 ± 0.05 to 1.60 ± 0.05 ‰; ~ 1.32 ‰; Fig. 6). Although there are currently no estimations for the Ni isotopic composition of the palaeo-ocean, the present-day global seawater $\delta^{60}\text{Ni}$ value has been constrained as 1.44 ± 0.15 ‰ (Cameron and Vance, 2014). This value lies within the $\delta^{60}\text{Ni}$ range of the marine sediments (Fig. 6; this study). Draw-down of Ni through the water column does not induce isotopic fractionation, and as such, the Ni stable isotope composition of the ocean is assumed to be homogenous (Cameron and Vance, 2014). However, the Ni stable isotope composition of the organic-rich sediments is far from homogenous, with $\delta^{60}\text{Ni}$ values that are either significantly lighter or heavier than the present-day seawater $\delta^{60}\text{Ni}$ value (Fig. 6). Assuming that global ocean homogeneity has persisted throughout geological time, the fractionation observed in the marine sediments must therefore be recording the

substantially variable isotopic compositions of the sources of dissolved Ni into the oceans.

This preliminary study presents Ni isotope and Ni concentration data from bulk sample analysis. To assess what fraction of the selected metals may be authigenic versus lithogenic, Table 4 presents Ni concentration data from this study, and from average shale and average upper continental crust. It is clear from this that the authigenic contribution of Ni in these samples is < 50 % (Table 4), suggesting that > 50 % of the sample is represented by the lithogenic fraction.

For both sample sets, no correlation is observed between $\delta^{60}\text{Ni}$ and Ni abundance, indicating that the level of Ni isotope fractionation in bulk marine sediments here is not directly controlled by the degree of Ni enrichment. Similarly, no relationship exists between $\delta^{60}\text{Ni}$ and redox for either sample set, suggesting that the level of isotopic fractionation is not solely dictated by the bottom water redox conditions at the time of sediment deposition. However, although it is currently poorly understood, it is interesting to consider whether or not the degree of organic matter preservation could have an effect on the observed isotopic fractionation within the sediments. The samples used for Ni isotope analysis across the Sinemurian-Pliensbachian boundary were deposited in predominantly oxic conditions (using the Ni/Co and V/Cr ratios). The tetrapyrrole complexes known to hold the majority of Ni in organic matter are poorly preserved under these conditions (Lewan and Maynard, 1982). As such, assuming break down of these complexes is heterogeneous, and that it does not result in the preferential loss of a particular isotope of Ni, this lack of preservation may at least partially contribute to the observed Ni isotope fractionation in these sediments.

In addition, no correlation is seen between $\delta^{60}\text{Ni}$ and TOC concentration in these samples, indicating that Ni isotope fractionation is not dependent on the concentration of organic matter in these sediments. However, all samples in this study have TOC contents of <3.0 wt. % (Table 3; apart from Exshaw Fm. sample SP10-10; 11.05 wt. %). As such, to further investigate the relationship between Ni fractionation and the organic carbon reservoir, work should be conducted on samples containing more varied and greater levels of TOC.

6.3. Fractionation of nickel stable isotopes in marine organic-rich sediments vs. terrestrial samples, extra-terrestrial samples and ferromanganese crusts

Marine sediments from the Exshaw Formation and Sinemurian-Pliensbachian GSSP yield a comparable range in $\delta^{60}\text{Ni}$ values (0.5-2.5 ‰ and 0.3-1.6 ‰, respectively; Fig. 6). Figure 6 compares these Ni isotopic values with that of bulk Earth and extraterrestrial samples (Cameron et al., 2009), including meteorites (0.2 ‰ to 0.4 ‰), basalts (0 to 0.3 ‰) and continental sediments (0 to 0.2 ‰). It is clear that these samples are significantly isotopically lighter than the organic-rich sediments (this study). In addition, Ni stable isotope fractionation occurs to a much greater degree in the sedimentary marine environment. Despite this though, there is minimal overlap between the $\delta^{60}\text{Ni}$ values for the organic-rich sediments and those of the abiotic terrestrial and extraterrestrial samples (Fig. 6).

The reasons for the heightened isotopic fractionation in marine sediments are currently poorly understood due to an extremely limited sample database. However, the complexity of the marine environment is likely to play a critical role in this. With assumed ocean isotopic homogeneity (Cameron and Vance, 2014), the

sources of dissolved Ni into seawater must exert a substantial control on the observed degree of isotopic fractionation. This may be partially attributed to the variability of the Ni isotope composition of the dissolved phase of rivers, which are a dominant source of Ni to the global oceans ($\delta^{60}\text{Ni} = 0.29$ to 1.34 ‰; Cameron and Vance, 2014). The heavier isotope composition of this fraction relative to silicates and continental sediments (0 ‰ to 0.3 ‰; Cameron et al., 2009) likely reflects isotopic fractionation induced by the weathering environment during riverine transport (Cameron and Vance, 2014).

However, this study demonstrates that the Ni isotopic composition of organic-rich marine sediments ($\delta^{60}\text{Ni} = 0.28$ to 2.50 ‰; this study) are significantly heavier than that of the riverine source (average $\delta^{60}\text{Ni} = 0.80$ ‰; Cameron and Vance, 2014). This is also the case for the dissolved phase of present-day seawater ($\delta^{60}\text{Ni} = 1.44 \pm 0.15$ ‰; Cameron and Vance, 2014). To reconcile this, there must therefore be either an additional input that is isotopically heavier than the riverine source (Cameron and Vance, 2014).

Dissolved trace metals are often removed from the water column via adsorption to mineral surfaces as they are incorporated into the sediment. The adsorption process, in particular to Mn and Fe oxyhydroxides, is known to induce isotopic fraction in a number of stable isotope systems, including Mo and U (Brennecke et al., 2011; Wasylenki et al., 2008; 2011). Sorption to Fe-Mn oxides is the main output of Ni from the oceans (Cameron and Vance, 2014), and more recently, this fractionation effect has also been revealed in the Ni stable isotope system (Wasylenki et al., 2014). In addition, experiments focusing on the adsorption and co-precipitation of Ni with oxyhydroxide phases (Wasylenki et al., 2014) have

demonstrated that isotopically light Ni is retained by these phases whilst isotopically heavy Ni is mobilised. This therefore leads to an enrichment of isotopically heavy Ni in the dissolved riverine load (Wasylenki et al., 2014).

Nickel stable isotope data for ferromanganese crusts (0.9-2.5 ‰; Gall et al., 2013) shows that their isotopic composition is comparable to that of the marine organic-rich sediments discussed herein. Following analysis of ferromanganese crusts in proximity to hydrothermal sources, Gall et al. (2013) suggest that hydrothermal fluids may have a Ni stable isotope composition of ~ 1.5 ‰. Thus hydrothermal sources may be contributing to the isotopic composition noted in the marine sediments herein.

However, both marine sediments (this study) and ferromanganese crusts (Gall et al., 2013) are at least in part recording isotopic fractionation from a source that is isotopically heavier than riverine and hydrothermal Ni influxes. As continental weathering is a primary source of Ni to the global oceans, it is likely that weathering-induced isotope fractionation could account for the isotopically heavy Ni composition of organic-rich marine sediments. Further, the heavy Ni isotope signature observed in these sediments may reflect the contribution of heavy dissolved Ni to the oceans following retention of the lighter Ni isotopes during weathering of oxyhydroxide phases (eg. Wasylenki et al., 2014). In support of this, analysis of ferromanganese crusts at varying distances from the continental shelf (Gall et al., 2013) demonstrates that crusts growing in proximity to a continental shelf contain the heaviest Ni isotope compositions. However, although weathering does affect the isotopic composition of marine sediments, the effects resulting from

additional factors such as riverine particulates and organic compounds have yet to be constrained (Cameron and Vance, 2014).

In addition, following examination of Ni isotope data from microorganisms ($\delta^{60}\text{Ni} = \sim 0.0$ to -1.6 ‰; Cameron et al., 2009), it can be noted that the Ni isotope ratios in the organic-rich sediments herein ($\delta^{60}\text{Ni} = \sim 0.28 - 2.50$ ‰) appear to have been driven in the opposite direction to those of the microorganisms. Whilst the causes of Ni isotope fractionation in these sediments are currently poorly understood, it appears that there is a fractionation effect associated with the Ni isotope system that may have parallels to the carbon isotope system, with the microorganisms taking up isotopically lighter Ni, thus potentially leaving behind an isotopically heavier Ni isotope signature in the sediment. Although it is impossible to draw a definitive conclusion from the current dataset, this study suggests that microorganisms and organic matter may play a key role in our understanding of Ni isotope fractionation (in a similar manner to the rhenium-osmium isotope system; Cumming et al., 2012; Harris et al., 2013) in organic-rich marine sediments, and as such, the importance of further investigation is emphasised.

7. Conclusions

This first investigation into the Ni stable isotope composition of organic-rich marine sediments from two distinct basins has yielded a number of key observations, outlined below.

533 1. This preliminary dataset indicates that organic-rich sediments have a Ni stable
 534 isotope composition ($\delta^{60}\text{Ni}$) of 0.28 to 2.50 ‰.

535 2. No relationship is observed between the Ni stable isotope composition of the
 536 organic-rich sediments and TOC, suggesting that fractionation is not determined by
 537 changes in the organic carbon reservoir.

538 3. Similarly, there is no correlation between $\delta^{60}\text{Ni}$ and Ni abundance or bottom-
 539 water redox conditions, suggesting that the process of Ni uptake and enrichment at
 540 the sediment-water interface, and the degree of oxygenation in the water-column
 541 do not exert primary control on isotopic fractionation.

542 4. The Ni isotope composition of marine sediments is substantially heavier and
 543 isotopically distinct to those of abiotic terrestrial and extraterrestrial samples ($\delta^{60}\text{N}$
 544 values of -0.1 to 0.3 ‰; Cameron et al., 2009).

545 5. Ni isotopes in marine sediments are isotopically heavier than those in present-day
 546 seawater and rivers ($\delta^{60}\text{Ni} = 1.44 \pm 0.15$ ‰ and 0.29 to 1.340 ‰, respectively;
 547 Cameron and Vance, 2014), indicating input of an isotopically heavier source of Ni to
 548 the ocean.

549 6. The observed range of $\delta^{60}\text{N}$ values in marine sediments is comparable to that of
 550 ferromanganese crusts (0.9 to 2.5 ‰; Gall et al., 2013). Adsorption of Ni to Fe-Mn
 551 oxyhydroxides results in the retention of isotopically light Ni and the mobilisation of
 552 isotopically heavier Ni during oxidative weathering (Wasylenki et al., 2014).
 553 Subsequently, the dissolved riverine load is enriched in heavier Ni. It is therefore
 554 probable that isotopic fractionation driven by the weathering environment plays a
 555 key role in yielding the range of $\delta^{60}\text{N}$ values that are observed in marine sediments.

7. The relatively heavy Ni stable isotope composition of marine sediments may also in part reflect influxes of dissolved Ni from hydrothermal sources ($\delta^{60}\text{Ni} = 1.5 \text{ ‰}$; Gall et al., 2013). However, further work is needed to investigate this.

The complexity of the sediment-seawater system may be the key factor that causes such enhanced levels of Ni isotope fractionation in marine sediments relative to meteorites, basalts and continental sediments. This preliminary dataset has produced some new and important data that can be the basis for further research of Ni in organic-rich marine sediments. As such, it is recommended that the relationships between Ni isotope fractionation and factors ubiquitous to the marine depositional system, such as bottom-water redox conditions, the type of organic matter present, organic matter preservation and TOC, are further explored.

Figure captions

Figure 1: Map and photograph showing the location of the Sinemurian-Pliensbachian GSSP section, Robin Hood's Bay, UK.

Figure 2: Graphic log showing the Sinemurian-Pliensbachian boundary GSSP and the relative locations of the samples analysed in this study. Samples used for Ni isotope analysis are in bold. Bed number classification taken from Hesselbo and Jenkyns (1995).

Figure 3: Present-day maturity map of the Exshaw Formation within Alberta, Canada (modified from Creaney and Allan, 1991). Map shows the location of the thermally immature, mature and overmature zones parallel to the Rocky Mountain Front, and the location of the well from which the core samples used in this study originate.

Figure 4: Nickel isotope ($\delta^{60}\text{Ni}$), Ni abundance, and TOC profiles for the Sinemurian-Pliensbachian section, presented against a corresponding stratigraphic column and graphic log. Black dashed line indicates the position of the Sinemurian-Pliensbachian boundary. ¹Bed numbers are from Hesselbo and Jenkyns (1995).

Figure 5: Plot showing the relationship between TOC and $\text{V}/(\text{V}+\text{Ni})$ for the Pennsylvanian Stark Shale Member samples (solid black squares) detailed in Hatch and Leventhal (1992), Robin Hood's Bay sediments (hollow diamonds; this study) and the Exshaw Formation shales (hollow triangles; this study). Black dashed lines mark the parameters discussed in Hatch and Leventhal (1992), whereby values of > 2.5 wt. % TOC correspond to $\text{V}/(\text{V}+\text{Ni})$ values > 0.75 for the Pennsylvanian Stark Shale Member.

Figure 6: Nickel stable isotope data for organic-rich marine sediments from Robin Hood's Bay, UK (RHB) and the Exshaw Formation. The grey box represents the average of the Ni isotope data for meteorites, basalts and continental sediments (~ 0.2 ‰ and 1 standard deviation either side of this; Cameron et al., 2009). The white circles show Ni isotope data from ferromanganese crusts (taken from Gall et al., 2013).

604

605 Table 1: Previously established values for the trace element ratios and their
606 corresponding depositional paleoredox conditions.

607

608 Table 2: Summary of trace element and TOC data and the associated ratios used for
609 paleoredox proxies, for the Robin Hood's Bay and Exshaw Formation marine
610 sediments.

611

612 Table 3: New nickel stable isotope data for a selection of Robin Hood's Bay and
613 Exshaw Formation marine sediments.

614

615 Table 4: A summary of elemental data for average shale, average upper continental
616 crust, Robin Hood's Bay and Exshaw Formation marine sediments.

617

618

619

620

621

622

623

624

625

626

627

628

629

630

631

632

633

634

635

636 **References**

637

638 Alberdi, M., and Lafargue, E., 1993, Vertical variations of organic matter content in
639 Guayuta Group (upper Cretaceous), Interior Mountain Belt, Eastern
640 Venezuela: Organic Geochemistry, v. 20, no. 4, p. 425-436.

641 Birck, J. L., and Lugmair, G. W., 1988, Nickel and chromium isotopes in Allende
642 inclusions: Earth and Planetary Science Letters, v. 90, no. 2, p. 131-143.

643 Brennecka, G. A., Wasylenki, L. E., Bargar, J. R., Weyer, S., and Anbar, A. D., 2011,
644 Uranium Isotope Fractionation during Adsorption to Mn-Oxyhydroxides:
645 Environmental Science and Technology, v. 45, no. 4, p. 1370-1375.

646 Cameron, V., Vance, D., Archer, C., and House, C. H., 2007, Nickel stable isotopes as
647 biogeochemical tracers, Goldschmidt Conference Abstracts, p. A141.

648 Cameron, V., Vance, D., Archer, C., and House, C. H., 2009, A biomarker based on the
649 stable isotopes of nickel: Proceedings of the National Academy of Sciences, v.
650 106, p. 10944-10948.

651 Cameron, V., Vance, D., and Poulton, S., 2011, Nickel isotopes, BIFs and the Archean
652 oceans, *Goldschmidt Conference Abstracts, Mineralogical Magazine*, p. 615.

653 Cameron, V., House, C. H., and Brantley, S. L., 2012, A First Analysis of Metallome
654 Biosignatures of Hyperthermophilic Archea: *Archea*, v. 2012, p. 1-12.

655 Cameron, V., and Vance, D., 2014, Heavy nickel isotope compositions in rivers and
656 the oceans, *Geochimica et Cosmochimica Acta*, v. 128, p. 195-211.

657 Caplan, M. L., and Bustin, R. M., 1998, Sedimentology and sequence stratigraphy of
658 Devonian-Carboniferous strata, southern Alberta: *Bulletin of Canadian*
659 *Petroleum Geology*, v. 46, p. 487-514.

660 Caplan, M. L., and Bustin, R. M., 1999, Palaeoceanographic controls on geochemical
661 characteristics of organic-rich Exshaw mudrocks: role of enhanced primary
662 production: *Organic Geochemistry*, v. 30, no. 2-3, p. 161-188.

663 Chen, J. H., Papanastassiou, D. A., and Wasserburg, G. J., 2009, A search for nickel
664 isotopic anomalies in iron meteorites and chondrites: *Geochimica et*
665 *Cosmochimica Acta*, v. 73, no. 5, p. 1461-1471.

666 Cook, D. L., Wadhwa, M., Clayton, R., Dauphas, N., Janney, P. E., and Davis, A. M.,
667 2007, Mass-dependent fractionation of nickel isotopes in meteoritic metal:
668 *Meteoritics and Planetary Science*, v. 42, no. 12, p. 2067-2077.

669 Creaney, S., and Allan, J., 1991, Hydrocarbon generation and migration in the
670 Western Canada sedimentary basin: *Geological Society, London, Special*
671 *Publications*, v. 50, no. 1, p. 189-202.

672 Creaser, R. A., Sannigrahi, P., Chacko, T., and Selby, D., 2002, Further evaluation of
673 the Re-Os geochronometer in organic-rich sedimentary rocks: a test of
674 hydrocarbon maturation effects in the Exshaw Formation, Western Canada

675 Sedimentary Basin: *Geochimica et Cosmochimica Acta*, v. 66, no. 19, p. 3441-
676 3452.

677 Cumming, V. M., Selby, D., and Lillis, P., 2012, Re-Os geochronology of the lacustrine
678 Green River Formation: Insights into direct depositional dating of lacustrine
679 successions, Re-Os systematics and paleocontinental weathering: *Earth and*
680 *Planetary Science Letters*, v. 359-360, p. 194-205.

681 Dean, W. T., Donovan, D. T., and Howarth, M. K., 1961, The Liassic ammonite Zones
682 and Subzones of the North West European Province: *Bulletin of the Natural*
683 *History Museum*, v. 4, p. 435-505.

684 Dera, G., Pucéat, E., Pellenard, P., Neige, P., Delsate, D., Joachimski, M. M., Reisberg,
685 L., and Martinez, M., 2009, Water mass exchange and variations in seawater
686 temperature in the NW Tethys during the Early Jurassic: Evidence from
687 neodymium and oxygen isotopes of fish teeth and belemnites: *Earth and*
688 *Planetary Science Letters*, v. 286, no. 1-2, p. 198-207.

689 Dewaker, K. N., Chandra, K., Arunachalam, J., and Karunasagar, D., 2000, Isotopic
690 fractionation of Ni⁶⁰/Ni⁶¹ in kerogen and bitumen samples: *Current Science*,
691 v. 79, no. 12, p. 1720-1723.

692 Dill, H., 1986, Metallogenesis of early Paleozoic graptolite shales from the
693 Graefenthal Horst (Northern Bavaria-Federal Republic of Germany):
694 *Economic Geology*, v. 81, p. 889-903.

695 Ellrich, J., Hirner, A., and Stärk, H., 1985, Distribution of trace elements in crude oils
696 from southern Germany: *Chemical Geology*, v. 48, no. 1-4, p. 313-323.

697 Frausto da Silva, J.J.R., and Williams, R.J.P., 2001, The Biological Chemistry of the
698 Elements: The Inorganic Chemistry of Life, Oxford University Press, Oxford, p.
699 436-449.

700 Gall, L., Williams, H., Siebert, C., and Halliday, A., 2012, Determination of mass-
701 dependent variations in nickel isotope compositions using double spiking and
702 MC-ICPMS: Journal of Analytical Atomic Spectrometry, v. 27, no. 1, p. 137-
703 145.

704 Gall, L., Williams, H. W., Siebert, C., Halliday, A. N., Herrington, R. J., and Hein, J. R.,
705 2013, Nickel isotopic compositions of ferromanganese crusts and the
706 constancy of deep ocean inputs and continental weathering effects over the
707 Cenozoic: Earth and Planetary Science Letters, v. 375, p. 148-155.

708 Gradstein, F. M., Ogg, J. G., Schmitz, M. D., and Ogg, G. M. 2012. The Geologic Time
709 Scale 2012. Elsevier.

710 Harris, N. B., Mnich, C. A., Selby, D., and Korn, D., 2013, Minor and trace element and
711 Re-Os chemistry of the Upper Devonian Woodford Shale, Permian Basin,
712 west Texas: Insights into metal abundance and basin processes: Chemical
713 Geology, v. 356, p. 76-93.

714 Hatch, J. R., and Leventhal, J. S., 1992, Relationship between inferred redox potential
715 of the depositional environment and geochemistry of the Upper
716 Pennsylvanian (Missourian) Stark Shale Member of the Dennis Limestone,
717 Wabaunsee County, Kansas, U.S.A: Chemical Geology, v. 99, no. 1-3, p. 65-82.

718 Herzog, G. F., hall, G. S., and Brownlee, D. E., 1994, Mass fractionation of nickel
719 isotopes in metallic cosmic spheres: Geochimica et Cosmochimica Acta, v. 58,
720 no. 23, p. 5319-5323.

721 Hesselbo, S. P., and Jenkyns, H. C., 1995, A comparison of the Hettangian to Bajocian
722 successions of Dorset and Yorkshire, *in* Taylor, P. D., ed., *Field Geology of the*
723 *British Jurassic*, Geological Society, London, p. 105-150.

724 Hesselbo, S. P., Meister, C., and Grocke, D. R., 2000, A potential global stratotype for
725 the Sinemurian-Pliensbachian boundary (Lower Jurassic), Robin Hood's Bay,
726 UK: ammonite faunas and isotope stratigraphy: *Geological Magazine*, v. 137,
727 no. 6, p. 601-607.

728 Jones, B., and Manning, D. A. C., 1994, Comparison of geochemical indices used for
729 the interpretation of palaeoredox conditions in ancient mudstones: *Chemical*
730 *Geology*, v. 111, no. 1-4, p. 111-129.

731 Jones, C. E., Jenkyns, H. C., and Hesselbo, S. P., 1994, Strontium isotopes in Early
732 Jurassic seawater: *Geochimica et Cosmochimica Acta*, v. 58, no. 4, p. 1285-
733 1301.

734 Kohman, T. P., and Robison, M. S., 1980, Iron-60 as a possible heat source and
735 chronometer in the early solar system: *Lunar and Planetary Science*, v. 11, p.
736 564-566.

737 Konhauser, K. O., Pecoits, E., Lalonde, S. V., Papineau, D., Nisbet, E. G., Barley, M. E.,
738 Arndt, N. T., Zahnle, K., and Kamber, B. S., 2009, Oceanic nickel depletion and
739 a methanogen famine before the Great Oxidation Event: *Nature*, v. 458, p.
740 750-753.

741 Leenheer, M. J., 1984, Mississippian Bakken and other equivalent formations as
742 source rocks in the Western Canada basin: *Organic Geochemistry*, v. 6, p.
743 521-533.

744 Lewan, M. D., 1984, Factors controlling the proportionality of vanadium to nickel in
 745 crude oils: *Geochimica et Cosmochimica Acta*, v. 48, no. 11, p. 2231-2238.

746 Lewan, M. D., and Maynard, J. B., 1982, Factors controlling enrichment of vanadium
 747 and nickel in the bitumen of organic sedimentary rocks: *Geochimica et*
 748 *Cosmochimica Acta*, v. 46, no. 12, p. 2547-2560.

749 Li, H.-Y., Schoonmaker, J., 2003, Chemical composition and mineralogy of marine
 750 sediments. In: *Treatise on Geochemistry. Sediments, Diagenesis, and*
 751 *Sedimentary Rocks*, v. 7, p. 1-35.

752 López, L., Lo Mónaco, S., Galarraga, F., Lira, A., and Cruz, C., 1995, VNi ratio in
 753 maltene and asphaltene fractions of crude oils from the west Venezuelan
 754 basin: correlation studies: *Chemical Geology*, v. 119, no. 1-4, p. 255-262.

755 Manning, L. K., Frost, C. D., and Branthaver, J. F., 1991, A neodymium isotopic study
 756 of crude oils and source rocks: potential applications for petroleum
 757 exploration: *Chemical Geology*, v. 91, no. 2, p. 125-138.

758 Meijer, N. C., Johnston, D. I., and Fullmer, E. G., 1994, Devonian stratigraphy and
 759 depositional history across Peace River Highland, west central Alberta and
 760 nearby British Columbia: *Geological Survey of Canada Open File 2851*, p. 40
 761 pp.

762 Meister, C., Aberhan, M., Blau, J., Dommergues, J.-L., Feist-Burkhardt, S., Hailwood,
 763 E. A., Hart, M., Hesselbo, S. P., Hounslow, M. W., Hylton, M., Morton, N.,
 764 Page, K., and Price, G. D., 2006, The Global Boundary Stratotype Section and
 765 Point (GSSP) for the base of the Pliensbachian Stage (Lower Jurassic), Wine
 766 Haven, Yorkshire, UK: *Episodes*, v. 29, no. 2, p. 93-114.

767 Morand, P., and Allègre, C. J., 1983, Nickel isotopic studies in meteorites: Earth and
 768 Planetary Science Letters, v. 63, no. 2, p. 167-176.

769 Moynier, F., Blichert-Toft, J., Telouk, P., Luck, J.-M., and Albarède, F., 2007,
 770 Comparative stable isotope geochemistry of Ni, Cu, Zn, and Fe in chondrites
 771 and iron meteorites: *Geochimica et Cosmochimica Acta*, v. 71, no. 17, p.
 772 4365-4379.

773 Ottley, C. J., Pearson, D. G., and Irvine, G. J., 2003, A routine method for the
 774 dissolution of geological samples for the analysis of REE and trace elements
 775 via ICP-MS, *in* Holland, G., and Tanner, S. D., eds., *Plasma source mass*
 776 *spectrometry: applications and emerging technologies*, p. 221-230.

777 Palmer, M. R., Kenison Falkner, K., Turekian, K. K., and Calvert, S. E., 1988, Sources of
 778 osmium isotopes in manganese nodules: *Geochimica et Cosmochimica Acta*,
 779 v. 52, no. 5, p. 1197-1202.

780 Peucker-Ehrenbrink, B., and Hannigan, R. E., 2000, Effects of black shale weathering
 781 on the mobility of rhenium and platinum group elements: *Geology*, v. 28, no.
 782 5, p. 475-478.

783 Piggott, N., and Lines, M. D., 1992, A case study of migration from the West Canada
 784 Basin, *in* England, W. A., and Fleet, A. J., eds., *Petroleum Migration, Volume*
 785 *59, Geological Society Special Publication*, p. 207-225.

786 Powell, J. H., 1984, Lithostratigraphical nomenclature of the Lias Group in the
 787 Yorkshire Basin: *Proceedings of the Yorkshire Geological Society*, v. 45, p. 51-
 788 57.

789 Quitté, G., Meier, M., Latkoczy, C., Halliday, A.N., and Günther, D., 2006, Nickel
 790 isotopes in iron meteorites—nucleosynthetic anomalies in sulphides with no

791 effects in metals and no trace of ^{60}Fe : Earth and Planetary Science Letters, v.
792 242, p. 16-25.

793 Quitté, G., and Oberli, F., 2006, Quantitative extraction and high precision isotope
794 measurements of nickel by MC-ICPMS: Journal of Analytical Atomic
795 Spectrometry, v. 21, p. 1249-1255.

796 Richards, B. C., and Higgins, A. C., 1988, Devonian-Carboniferous beds of the Palliser
797 and Exshaw formations at Jura Creekm Rocky Mountains, southwestern
798 Alberta, *in* McMillan, N. J., ed., Devonian of the world, Canadian Society of
799 Petroleum Geologists Memoir, Volume 14, p. 399-412.

800 Richards, B. C., Mamet, B. L., and Bamber, E. W., 1999, Uppermost Devonian and
801 Carboniferous sequence stratigraphy, biostratigraphy and basin
802 development, Banff region, southwestern Alberta, XIV International Congress
803 on the Carboniferous and Permian, Field Trip, 4-7 and 4-17 Guidebook:
804 Calgary, Alberta.

805 Richards, C., Ross, G. M., and Utting, J., 2002, U-Pb geochronology, lithostratigraphy
806 and biostratigraphy of tuff in the Upper Famennian to Tournaisian Exshaw
807 Formation: Evidence for a mid-Paleozoic magmatic arc on the northwestern
808 margin of North America, *in* Hills, L. V., Henderson, C. M., and Bamber, E. W.,
809 eds., Carboniferous and Permian of the World: XIV ICCP Proceedings, Volume
810 19, Can Soc Petrol Geol Mem, p. 158-207.

811 Rimmer, S. M., 2004, Geochemical paleoredox indicators in Devonian-Mississippian
812 black shales, Central Appalachian Basin (USA), Chemical Geology, v. 206, no.
813 3-4, p. 373-391.

814 Rudnick, R. L., and Gao, S., 2003, 3.01 Composition of the Continental Crust: Treatise
815 on Geochemistry, v. 3, p. 1-64.

816 Schovsbo, N. H., 2001, Why barren intervals? A taphonomic case study of the
817 Scandinavian Alum Shale and its faunas: *Lethaia*, v. 34, no. 4, p. 271-285.

818 Sclater, F., Boyle, E., Edmond, J., 1976, On the marine geochemistry of nickel: *Earth*
819 *and Planetary Science Letters*, v. 31, p. 119-128.

820 Selby, D., and Creaser, R. A., 2005, Direct radiometric dating of the Devonian-
821 Mississippian time-scale boundary using the Re-Os black shale
822 geochronometer: *Geology*, v. 33, p. 545-548.

823 Selby, D., Mutterlose, J., and Condon, D. J., 2009, U-Pb and Re-Os geochronology of
824 the Aptian/Albian and Cenomanian/Turonian stage boundaries: Implications
825 for timescale calibration, osmium isotope seawater composition and Re-Os
826 systematics in organic-rich sediments: *Chemical Geology*, v. 265, no. 3-4, p.
827 394-409.

828 Sellwood, B. W., and Jenkyns, H. C., 1975, Basins and swells and the evolution of an
829 epeiric sea (Pliensbachian-Bajocian of Great Britain): *Journal of the Geological*
830 *Society*, v. 131, no. 4, p. 373-388.

831 Shimamura, T., and Lugmair, G. W., 1983, Ni isotopic compositions in Allende and
832 other meteorites: *Earth and Planetary Science Letters*, v. 63, no. 2, p. 177-
833 188.

834 Spath, L. F., 1923, Correlation of the Ibex and Jamesoni Zones of the Lower Lias:
835 *Geological Magazine*, v. 60, p. 6-11.

836 Wasylenki, L., Spivak-Birndorf, L., Howe, H., and Wells, R., 2014, Experiments reveal
837 the mechanism by which Ni isotopes fractionate in the weathering
838 environment: *Goldschmidt Abstracts*, 2661.

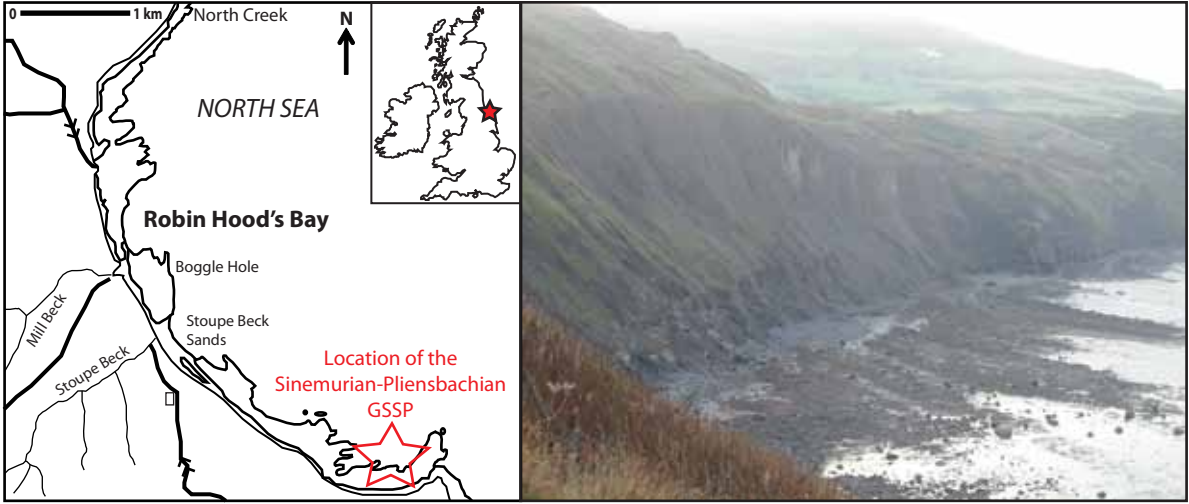
839 Wasylenki, L. E., Rolfe, B. A., Weeks, C. L., Spiro, T. G., and Anbar, A. D., 2008,
840 Experimental investigation of the effects of temperature and ionic strength
841 on Mo isotope fractionation during adsorption to manganese oxides:
842 *Geochimica et Cosmochimica Acta*, v. 72, p. 5997-6005.

843 Wasylenki, L. E., Weeks, C. L., Bargar, J. R., Spiro, T. G., Hein, J. R., and Anbar, A. D.,
844 2011, The molecular mechanism of Mo isotope fractionation during
845 adsorption to birnessite: *Geochimica et Cosmochimica Acta*, v. 75, no. 17, p.
846 5019-5031.

847 Wedepohl, K. H., 1971, Environmental influences on the chemical composition of
848 shales and clays: *Physics and Chemistry of the Earth*, v. 8, p. 305-333.

849 Xue, S., Herzog, G. F., Hall, G. S., Klein, J., Middleton, R., and Juenemann, D., 1995,
850 Stable nickel isotopes and cosmogenic beryllium-10 and aluminum-26 in
851 metallic spheroids from Meteor Crater, Arizona: *Meteoritics*, v. 30, p. 303-
852 310.

Figure 1



[illegible]

Figure 3

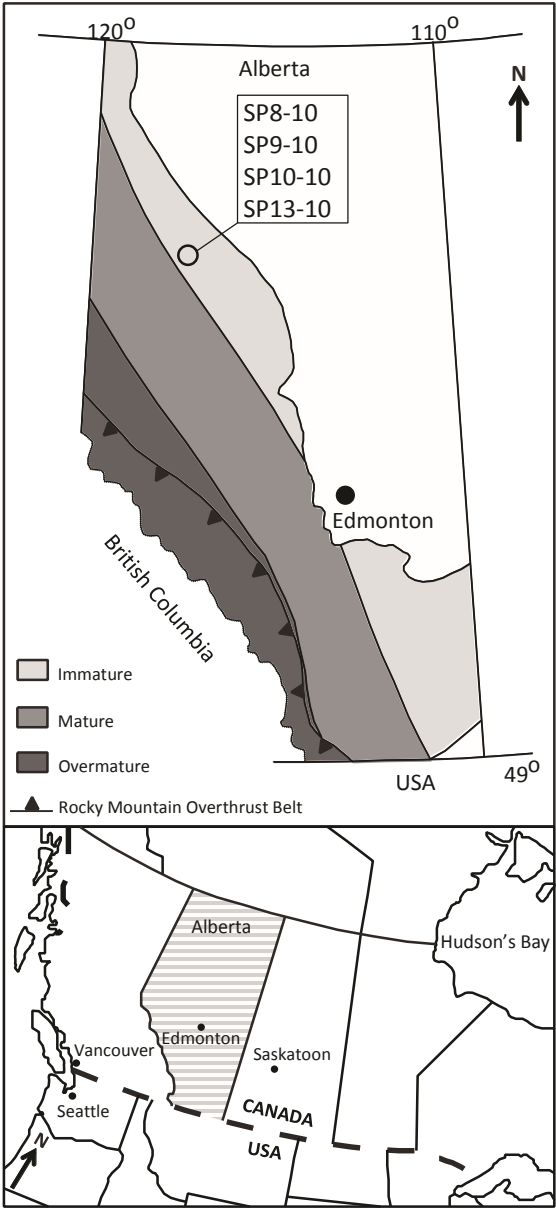


Figure 4

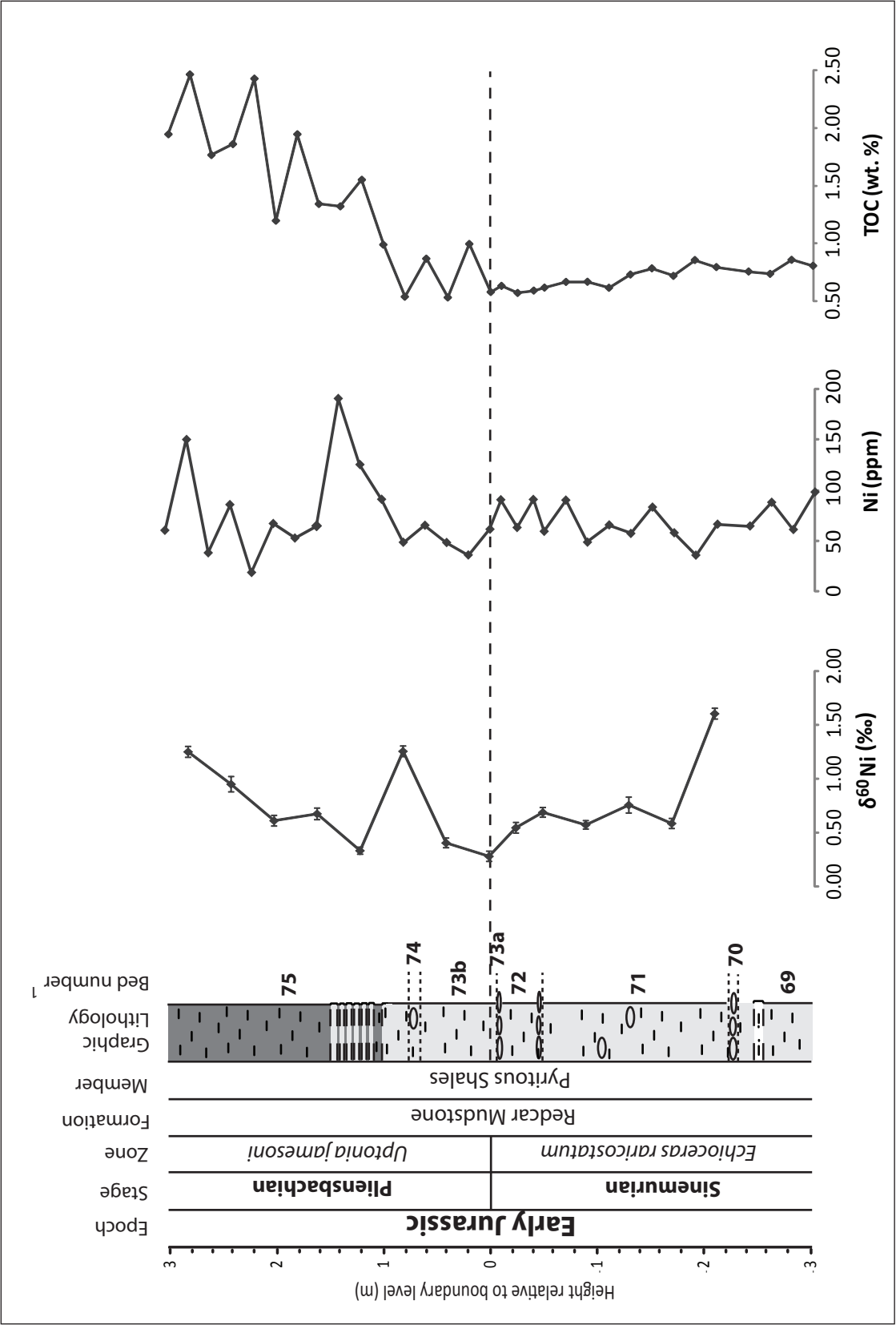


Figure 5

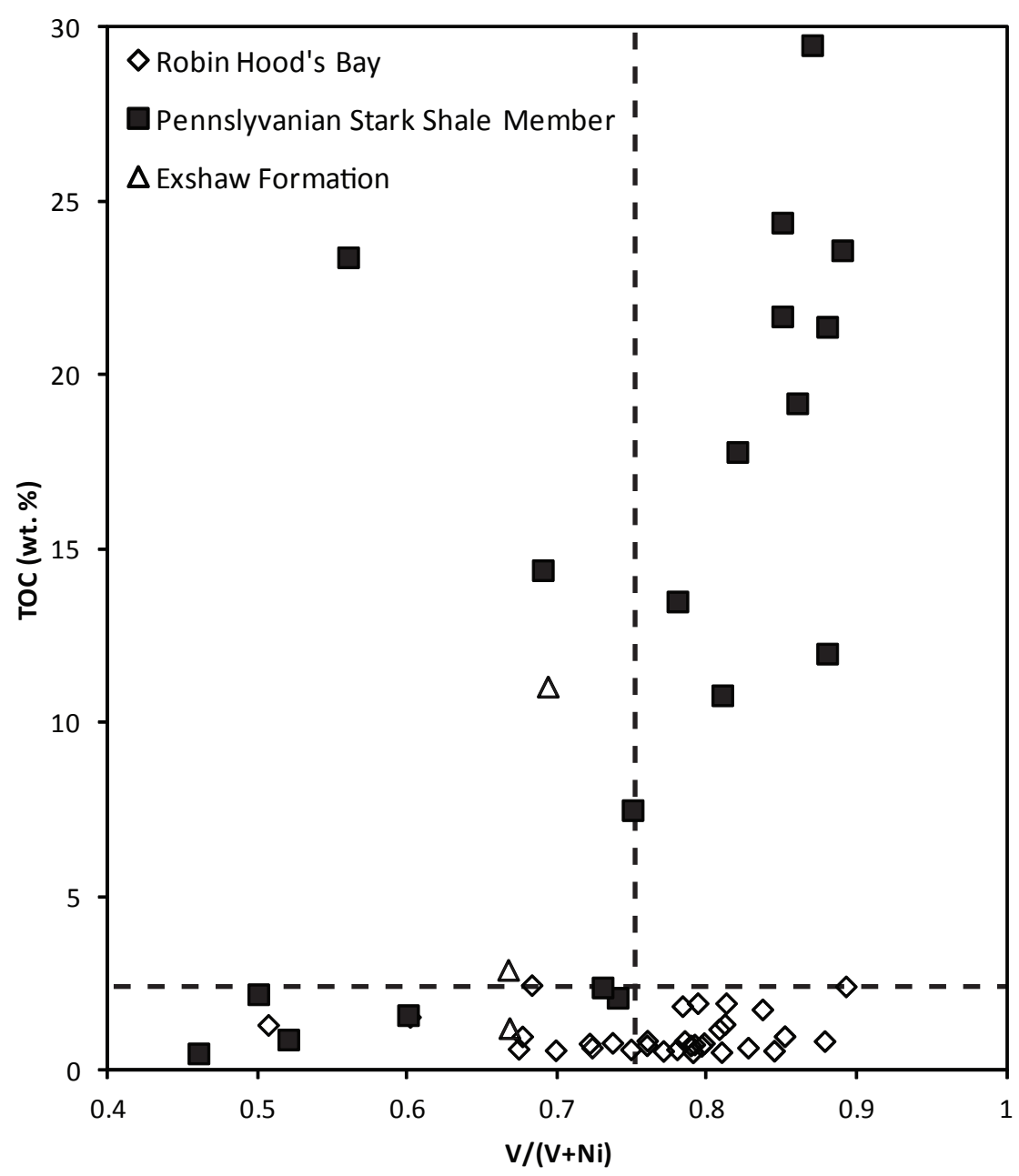


Figure 6

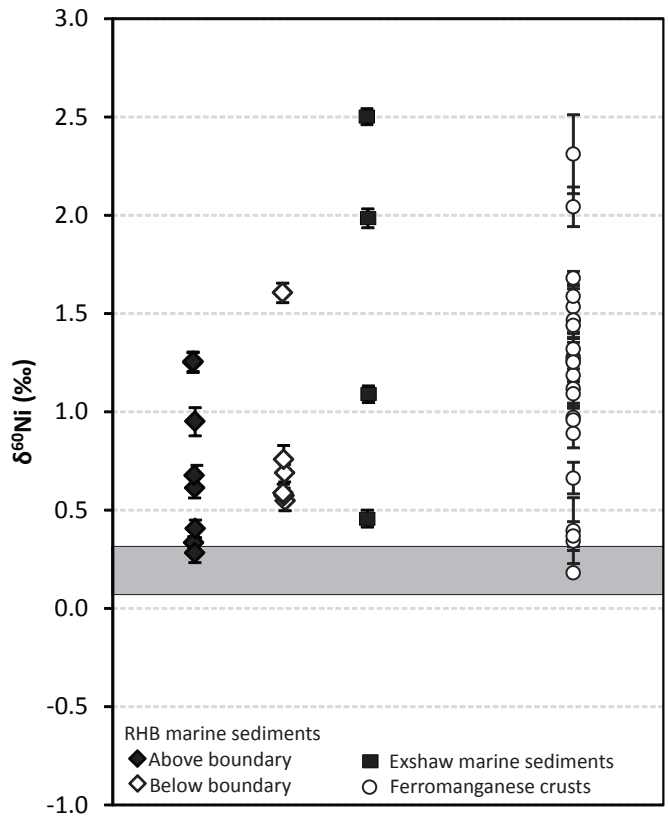


Table 1
[Click here to download Table: Table 1 Redox parameters.pdf](#)

	Oxic	Dysoxic	Suboxic-anoxic	Euxinic
V/Cr ^a	<2.00	2.00-4.25	>4.25	
Ni/Co ^a	<5.00	5.00-7.00	>7.00	
V/(V+Ni) ^b		0.46-0.60	0.54-0.82	>0.84

^a Jones and Manning (1994)

^b Hatch and Leventhal (1992); Schovsbo (2001)

Table 2
Click here to download Table: Table 2 Trace element data.pdf

Sample	Distance from S-P boundary (m) ^a	Depth (m) ^b	Trace elements (ppm)				Redox ratios			TOC (wt. %)
			V	Cr	Ni	Co	V/Cr	Ni/Co	V/(V+Ni)	
Robin Hood's Bay, UK										
SP37-09	3.0		230.9	130.6	60.11	26.87	1.77	2.24	0.79	1.94
SP36-09	2.8		322.4	148.2	149.9	24.70	2.18	6.07	0.68	2.46
SP35-09	2.6		194.0	107.6	37.86	18.95	1.80	2.00	0.84	1.76
SP34-09	2.4		309.3	134.5	85.57	19.82	2.30	4.32	0.78	1.86
SP33-09	2.2		152.9	107.5	18.43	12.88	1.42	1.43	0.89	2.43
SP32-09	2.0		280.8	147.3	66.81	16.21	1.91	4.12	0.81	1.20
SP31-09	1.8		227.3	130.9	52.47	20.46	1.74	2.56	0.81	1.94
SP30-09	1.6		277.7	146.9	64.49	16.37	1.89	3.94	0.81	1.34
SP29-09	1.4		195.6	158.7	190.5	20.61	1.23	9.24	0.51	1.32
SP28-09	1.2		188.8	120.2	125.2	34.40	1.57	3.64	0.60	1.55
SP27-09	1.0		189.8	148.2	90.83	21.69	1.28	4.19	0.68	0.99
SP26-09	0.8		204.9	133.4	48.25	16.55	1.54	2.92	0.81	0.54
SP25-09	0.6		205.8	130.1	65.09	22.05	1.58	2.95	0.76	0.87
SP24-09	0.4		181.1	142.6	48.06	17.63	1.27	2.73	0.79	0.53
SP23-09	0.2		204.8	120.1	35.70	19.10	1.71	1.87	0.85	0.99
SP22-09	0.0		332.6	276.8	61.23	18.45	1.20	3.32	0.84	0.58
SP38-09	-0.1		186.7	165.8	90.33	20.09	1.13	4.50	0.67	0.63
SP21-09	-0.3		211.1	122.5	62.86	20.41	1.72	3.08	0.77	0.57
SP39-09	-0.4		210.1	154.5	90.66	20.83	1.36	4.35	0.70	0.59
SP20-09	-0.5		209.2	135.9	59.13	15.35	1.54	3.85	0.78	0.62
SP19-09	-0.7		234.8	164.9	90.00	25.73	1.42	3.50	0.72	0.67
SP18-09	-0.9		231.6	142.8	48.40	18.42	1.62	2.63	0.83	0.67
SP17-09	-1.1		195.1	133.8	65.42	25.03	1.46	2.61	0.75	0.61
SP16-09	-1.3		213.1	132.0	57.04	20.22	1.62	2.82	0.79	0.73
SP15-09	-1.5		214.8	129.9	83.02	25.72	1.65	3.23	0.72	0.78
SP14-09	-1.7		225.0	133.1	57.69	17.88	1.69	3.23	0.80	0.72
SP13-09	-1.9		256.4	127.2	35.53	15.94	2.02	2.23	0.88	0.86
SP12-09	-2.1		261.0	142.8	66.18	23.19	1.83	2.85	0.80	0.79
SP8-09	-2.3		244.2	136.2	64.39	22.01	1.79	2.93	0.79	0.76
SP9-09	-2.6		277.4	140.3	87.84	21.88	1.98	4.01	0.76	0.74
SP10-09	-2.8		222.0	146.7	60.89	21.79	1.51	2.79	0.78	0.86
SP11-09	-3.0		273.9	139.0	97.97	18.88	1.97	5.19	0.74	0.81
Exshaw Formation, Canada ^c										
SP8-10		1753	108.7	53.5	3.75	54.08	2.03	14.42	0.67	1.23
SP9-10		1754	40.3	19.5	3.75	80.14	2.07	21.37	0.33	1.99
SP10-10		1756.2	350.2	38.9	11.25	154.88	9.00	13.77	0.69	11.05
SP13-10		1756.5	132.8	18.5	4.11	66.33	7.17	16.15	0.67	2.90

^a Parameter only applicable to Robin Hood's Bay samples
^b Parameter only applicable to Exshaw Formation samples
^c All samples are thermally immature and from core 3-19-80-23W5

Table 3
Click here to download Table: Table 3 Ni isotope data.pdf

	Distance from S-P boundary					
Sample ID	(m) ^a	Depth (m) ^b	$\delta^{60}\text{Ni}$ (‰)		2 σ	Ni (ppm)
<i>Robin Hood's Bay, UK</i>						
SP36-09	2.8		1.25	±	0.05	149.92
SP34-09	2.4		0.95	±	0.07	85.57
SP32-09	2		0.61	±	0.05	66.81
SP30-09	1.6		0.67	±	0.05	64.49
SP28-09	1.2		0.33	±	0.03	125.18
SP26-09	0.8		1.26	±	0.05	48.25
SP24-09	0.4		0.40	±	0.05	48.06
SP22-09	0		0.28	±	0.05	61.23
SP21-09	-0.25		0.55	±	0.05	62.86
SP20-09	-0.5		0.69	±	0.04	59.13
SP18-09	-0.9		0.57	±	0.04	48.40
SP16-09	-1.3		0.76	±	0.07	57.04
SP14-09	-1.7		0.58	±	0.05	57.69
SP12-09	-2.1		1.60	±	0.05	66.18
<i>Exshaw Formation, Canada^c</i>						
SP8-10		1753	1.09	±	0.04	54.1
SP9-10		1754	1.98	±	0.05	80.1
SP10-10		1756.2	0.46	±	0.04	154.9
SP13-10		1756.5	2.50	±	0.04	66.3

^a Parameter only applicable to Robin Hood's Bay samples
^b Parameter only applicable to Exshaw Formation samples
^c All samples are thermally immature and from core 3-19-80-23W5

Table 4
[Click here to download Table: Table 4 Elemental summary.pdf](#)

Element (ppm)	Average shale ^a	Average		
		Upper Crust ^b	This Study ^c	This study ^d
Ni	68	47	18-190	54-154
Co	19	17	3-11	12-34
V	130	97	152-332	40-350
Cr	90	92	107-268	18-53

^a Average shale values from Wedepohl (1971)

^b Average upper continental crust values from Rudnick and Gao (2003)

^c Samples from Robin Hood's Bay, UK

^d Samples from the Exshaw Formation, Canada